



*Supplement of*

## **Unveiling the optimal regression model for source apportionment of the oxidative potential of PM<sub>10</sub>**

Vy Dinh Ngoc Thuy et al.

*Correspondence to:* Gaëlle Uzu (gaelleuzu@ird.fr)

The copyright of individual parts of the supplement might differ from the article licence.

## OP activities in cold and warm periods

Table S. 1.  $\text{PM}_{10}$  OP<sub>AA</sub> and  $\text{PM}_{10}$  OP<sub>DTT</sub> values in cold (Jan, Feb, Mar, Oct, Nov, Dec) and warm (Apr, May, Jun, Jul, Aug, Sep) periods (in  $\text{nmol} \cdot \text{min}^{-1} \cdot \text{m}^{-3}$ )

	<b>PdB</b>	<b>TAL</b>	<b>GRE-fr</b>	<b>CHAM</b>	<b>RBX</b>	<b>NIC</b>
<b>Cold OP<sub>AA</sub></b>	0.86±0.16	1.6±0.23	2.35±0.62	4.11±1.28	2.74±0.51	1.38±0.38
<b>Warm OP<sub>AA</sub></b>	0.38±0.17	0.48±0.28	0.74±0.36	0.72±0.41	1.68±0.43	0.68±0.19
<b>Cold OP<sub>DTT</sub></b>	1.97±0.16	2.24±0.48	1.83±0.51	3.36±0.52	2.78±0.67	2.61±0.36
<b>Warm OP<sub>DTT</sub></b>	1.64±0.29	1.47±0.38	1.29±0.34	1.48±0.24	2.51±0.52	2.14±0.4

## The VIF values of PM sources

Table S.2. The VIF values of PM sources

<b>Sources</b>	<b>PdB</b>	<b>TAL</b>	<b>GRE-fr</b>	<b>CHAM</b>	<b>RBX</b>	<b>NIC</b>
<b>Aged salt</b>	2.64	2.09	2.44		2.19	2.65
<b>Biomass burning</b>	2.14	3.74	4.29	3.43	2.11	2.48
<b>Dust</b>	2.47	2.54	2.50	2.08	2.17	2.80
<b>HFO</b>	2.53					
<b>Industrial</b>	1.90	3.18	1.87			
<b>MSA rich</b>	2.68	1.83	1.85	1.98	1.94	2.92
<b>Nitrate rich</b>	2.30	1.55	2.13	2.08	2.93	2.23
<b>Primary biogenic</b>	2.22	2.12	2.13	2.93	1.73	2.34
<b>Salt</b>	1.80	1.38	2.41	1.84	1.74	1.82
<b>Sulfate rich</b>	2.51	2.54	3.49	2.89	2.64	2.90
<b>Road traffic</b>		4.45	3.02	4.42	1.96	4.56

## Relationships between the regression analysis residuals and the fitted values

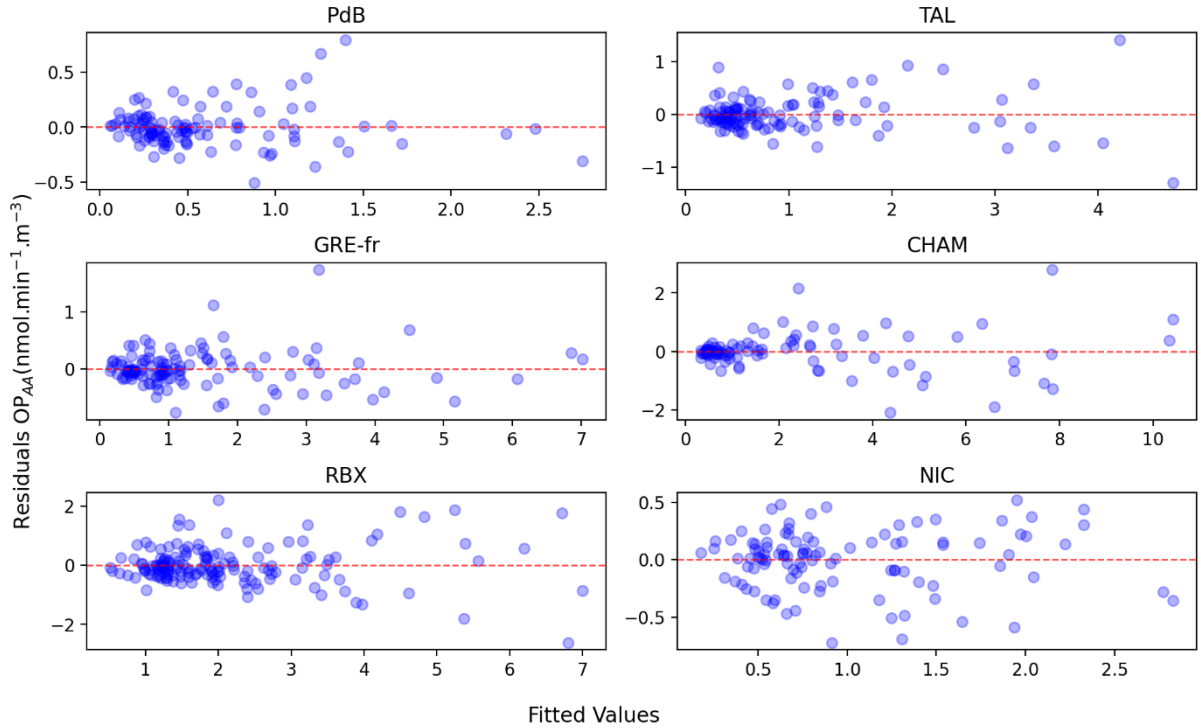


Figure S.1. Relationships between the regression analysis residuals and the fitted values for  $\text{PM}_{10} OP_{AA}$

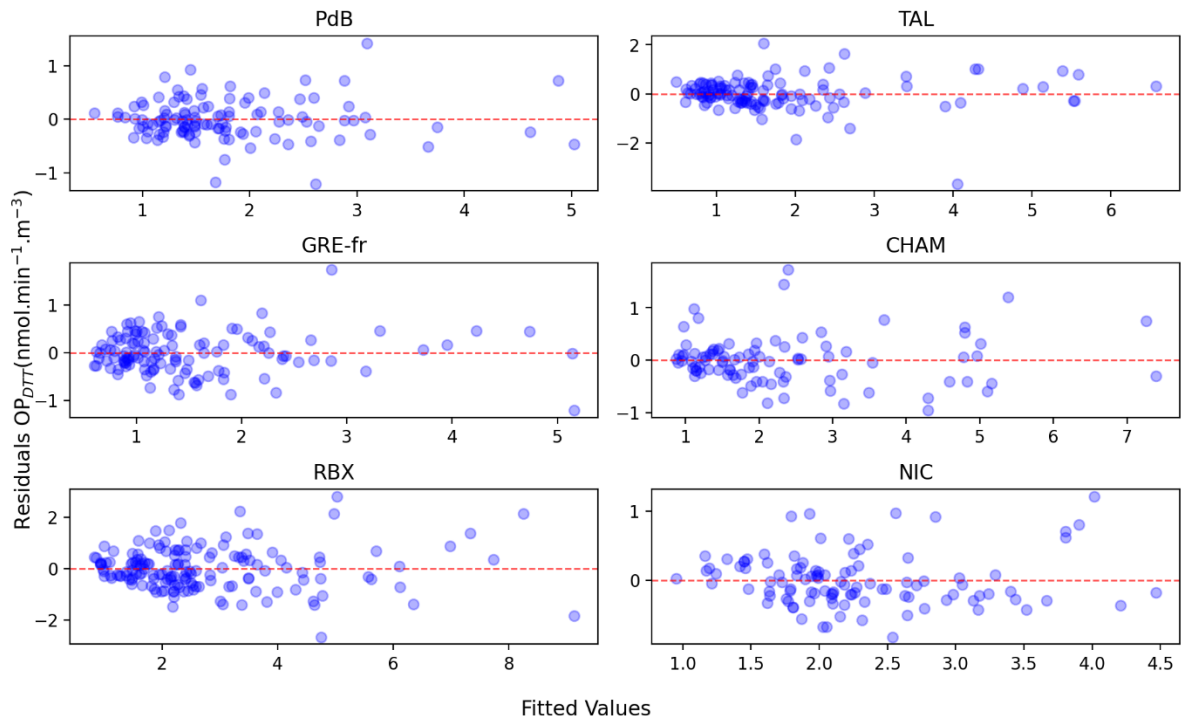


Figure S.2. Relationships between the regression analysis residuals and the fitted values for  $\text{PM}_{10} OP_{DTT}$

## Performance metric results

Table S. 3.  $R^2$  (mean  $\pm$  std ) of the training and testing datasets of all models in  $PM_{10}OP_{AA}$  and  $PM_{10}OP_{DTT}$  prediction

OPtype	Methods	PdB_test	PdB_train	TAL_test	TAL_train	GRE-fr_test	GRE-fr_train	CHAM_test	CHAM_train	RBX_test	RBX_train	NIC_test	NIC_train
AA	<b>OLS</b>	0.75 $\pm$ 0.18	0.87 $\pm$ 0.02	0.77 $\pm$ 0.13	0.87 $\pm$ 0.01	0.9 $\pm$ 0.08	0.95 $\pm$ 0.01	0.87 $\pm$ 0.08	0.93 $\pm$ 0.01	0.63 $\pm$ 0.16	0.75 $\pm$ 0.03	0.7 $\pm$ 0.16	0.81 $\pm$ 0.02
	<b>WLS</b>	0.72 $\pm$ 0.24	0.86 $\pm$ 0.03	0.67 $\pm$ 0.26	0.8 $\pm$ 0.05	0.9 $\pm$ 0.08	0.94 $\pm$ 0.01	0.85 $\pm$ 0.1	0.89 $\pm$ 0.02	0.65 $\pm$ 0.13	0.73 $\pm$ 0.03	0.74 $\pm$ 0.13	0.82 $\pm$ 0.02
	<b>wPLS</b>	0.74 $\pm$ 0.2	0.86 $\pm$ 0.03	0.68 $\pm$ 0.25	0.8 $\pm$ 0.04	0.9 $\pm$ 0.08	0.93 $\pm$ 0.02	0.85 $\pm$ 0.12	0.89 $\pm$ 0.02	0.66 $\pm$ 0.13	0.73 $\pm$ 0.03	0.76 $\pm$ 0.12	0.82 $\pm$ 0.02
	<b>PLS</b>	0.76 $\pm$ 0.17	0.86 $\pm$ 0.02	0.78 $\pm$ 0.13	0.87 $\pm$ 0.01	0.9 $\pm$ 0.08	0.94 $\pm$ 0.01	0.88 $\pm$ 0.08	0.93 $\pm$ 0.01	0.64 $\pm$ 0.17	0.75 $\pm$ 0.03	0.73 $\pm$ 0.14	0.8 $\pm$ 0.02
	<b>wRidge</b>	0.72 $\pm$ 0.24	0.86 $\pm$ 0.03	0.67 $\pm$ 0.26	0.8 $\pm$ 0.05	0.9 $\pm$ 0.08	0.94 $\pm$ 0.01	0.85 $\pm$ 0.1	0.89 $\pm$ 0.02	0.65 $\pm$ 0.13	0.73 $\pm$ 0.03	0.74 $\pm$ 0.13	0.82 $\pm$ 0.02
	<b>Ridge</b>	0.75 $\pm$ 0.18	0.87 $\pm$ 0.02	0.77 $\pm$ 0.13	0.87 $\pm$ 0.01	0.9 $\pm$ 0.08	0.95 $\pm$ 0.01	0.87 $\pm$ 0.08	0.93 $\pm$ 0.01	0.63 $\pm$ 0.16	0.75 $\pm$ 0.03	0.7 $\pm$ 0.16	0.81 $\pm$ 0.02
	<b>wLasso</b>	0.71 $\pm$ 0.26	0.84 $\pm$ 0.03	0.66 $\pm$ 0.28	0.78 $\pm$ 0.05	0.84 $\pm$ 0.14	0.9 $\pm$ 0.03	0.84 $\pm$ 0.11	0.88 $\pm$ 0.02	0.65 $\pm$ 0.13	0.73 $\pm$ 0.04	0.74 $\pm$ 0.13	0.81 $\pm$ 0.02
	<b>Lasso</b>	0.74 $\pm$ 0.19	0.86 $\pm$ 0.02	0.78 $\pm$ 0.13	0.87 $\pm$ 0.01	0.9 $\pm$ 0.08	0.95 $\pm$ 0.01	0.87 $\pm$ 0.08	0.93 $\pm$ 0.01	0.63 $\pm$ 0.17	0.74 $\pm$ 0.03	0.7 $\pm$ 0.16	0.8 $\pm$ 0.02
	<b>GLM</b>	0.21 $\pm$ 0.58	0.74 $\pm$ 0.04	0.19 $\pm$ 0.59	0.79 $\pm$ 0.04	0.59 $\pm$ 0.3	0.86 $\pm$ 0.02	0.77 $\pm$ 0.19	0.9 $\pm$ 0.02	0.26 $\pm$ 0.48	0.64 $\pm$ 0.06	0.51 $\pm$ 0.4	0.76 $\pm$ 0.03
	<b>RF</b>	0.55 $\pm$ 0.26	0.95 $\pm$ 0.01	0.68 $\pm$ 0.27	0.96 $\pm$ 0.01	0.8 $\pm$ 0.13	0.97 $\pm$ 0.01	0.78 $\pm$ 0.21	0.97 $\pm$ 0.01	0.27 $\pm$ 0.39	0.92 $\pm$ 0.02	0.61 $\pm$ 0.23	0.95 $\pm$ 0.01
	<b>MLP</b>	0.52 $\pm$ 0.63	0.82 $\pm$ 0.21	0.69 $\pm$ 0.23	0.87 $\pm$ 0.09	0.81 $\pm$ 0.2	0.91 $\pm$ 0.06	0.85 $\pm$ 0.11	0.91 $\pm$ 0.04	0.48 $\pm$ 0.31	0.69 $\pm$ 0.21	0.59 $\pm$ 0.23	0.78 $\pm$ 0.14
DTT	<b>OLS</b>	0.71 $\pm$ 0.17	0.83 $\pm$ 0.03	0.62 $\pm$ 0.29	0.76 $\pm$ 0.06	0.73 $\pm$ 0.17	0.83 $\pm$ 0.03	0.81 $\pm$ 0.14	0.9 $\pm$ 0.02	0.61 $\pm$ 0.18	0.74 $\pm$ 0.03	0.65 $\pm$ 0.16	0.78 $\pm$ 0.02
	<b>WLS</b>	0.69 $\pm$ 0.18	0.81 $\pm$ 0.03	0.56 $\pm$ 0.31	0.69 $\pm$ 0.09	0.46 $\pm$ 0.39	0.66 $\pm$ 0.1	0.79 $\pm$ 0.19	0.87 $\pm$ 0.02	0.54 $\pm$ 0.27	0.66 $\pm$ 0.06	0.61 $\pm$ 0.17	0.72 $\pm$ 0.04
	<b>wPLS</b>	0.69 $\pm$ 0.18	0.81 $\pm$ 0.03	0.61 $\pm$ 0.29	0.71 $\pm$ 0.08	0.43 $\pm$ 0.47	0.62 $\pm$ 0.14	0.79 $\pm$ 0.19	0.87 $\pm$ 0.02	0.57 $\pm$ 0.22	0.65 $\pm$ 0.06	0.62 $\pm$ 0.17	0.72 $\pm$ 0.04
	<b>PLS</b>	0.71 $\pm$ 0.17	0.83 $\pm$ 0.03	0.63 $\pm$ 0.29	0.76 $\pm$ 0.06	0.73 $\pm$ 0.17	0.83 $\pm$ 0.03	0.81 $\pm$ 0.14	0.9 $\pm$ 0.02	0.61 $\pm$ 0.17	0.72 $\pm$ 0.03	0.65 $\pm$ 0.16	0.78 $\pm$ 0.02
	<b>wRidge</b>	0.69 $\pm$ 0.18	0.81 $\pm$ 0.03	0.56 $\pm$ 0.31	0.69 $\pm$ 0.09	0.46 $\pm$ 0.39	0.66 $\pm$ 0.1	0.79 $\pm$ 0.19	0.87 $\pm$ 0.02	0.54 $\pm$ 0.27	0.66 $\pm$ 0.06	0.61 $\pm$ 0.17	0.72 $\pm$ 0.04
	<b>Ridge</b>	0.71 $\pm$ 0.17	0.83 $\pm$ 0.03	0.62 $\pm$ 0.29	0.76 $\pm$ 0.06	0.73 $\pm$ 0.17	0.83 $\pm$ 0.03	0.81 $\pm$ 0.14	0.9 $\pm$ 0.02	0.61 $\pm$ 0.18	0.74 $\pm$ 0.03	0.65 $\pm$ 0.16	0.78 $\pm$ 0.02
	<b>wLasso</b>	0.67 $\pm$ 0.19	0.8 $\pm$ 0.03	0.54 $\pm$ 0.32	0.68 $\pm$ 0.1	0.21 $\pm$ 0.64	0.47 $\pm$ 0.23	0.76 $\pm$ 0.21	0.86 $\pm$ 0.03	0.55 $\pm$ 0.26	0.66 $\pm$ 0.06	0.57 $\pm$ 0.19	0.69 $\pm$ 0.04
	<b>Lasso</b>	0.7 $\pm$ 0.17	0.82 $\pm$ 0.03	0.62 $\pm$ 0.29	0.76 $\pm$ 0.06	0.73 $\pm$ 0.17	0.82 $\pm$ 0.03	0.8 $\pm$ 0.14	0.9 $\pm$ 0.02	0.6 $\pm$ 0.18	0.74 $\pm$ 0.03	0.64 $\pm$ 0.18	0.77 $\pm$ 0.02
	<b>GLM</b>	0.56 $\pm$ 0.32	0.8 $\pm$ 0.03	0.33 $\pm$ 0.71	0.75 $\pm$ 0.05	0.32 $\pm$ 0.62	0.72 $\pm$ 0.04	0.67 $\pm$ 0.38	0.86 $\pm$ 0.02	0.21 $\pm$ 0.6	0.64 $\pm$ 0.07	0.65 $\pm$ 0.18	0.81 $\pm$ 0.03
	<b>RF</b>	0.1 $\pm$ 0.54	0.92 $\pm$ 0.02	0.42 $\pm$ 0.43	0.93 $\pm$ 0.02	0.37 $\pm$ 0.39	0.93 $\pm$ 0.02	0.55 $\pm$ 0.32	0.95 $\pm$ 0.01	0.42 $\pm$ 0.3	0.93 $\pm$ 0.01	-0.13 $\pm$ 0.79	0.9 $\pm$ 0.03
	<b>MLP</b>	0.48 $\pm$ 0.34	0.75 $\pm$ 0.13	0.5 $\pm$ 0.36	0.77 $\pm$ 0.11	0.59 $\pm$ 0.25	0.77 $\pm$ 0.11	0.73 $\pm$ 0.18	0.85 $\pm$ 0.09	0.56 $\pm$ 0.26	0.73 $\pm$ 0.12	0.54 $\pm$ 0.25	0.69 $\pm$ 0.12

Table S. 4. MAE (mean  $\pm$  std ) of the training and testing datasets of all models in  $\text{PM}_{10}\text{OP}_{\text{AA}}$  and  $\text{PM}_{10}\text{OP}_{\text{DTT}}$  prediction

OPtype	Methods	PdB_test	PdB_train	TAL_test	TAL_train	GRE-fr_test	GRE-fr_train	CHAM_test	CHAM_train	RBX_test	RBX_train	NIC_test	NIC_train
AA	<b>OLS</b>	0.15 $\pm$ 0.03	0.12 $\pm$ 0.01	0.26 $\pm$ 0.05	0.23 $\pm$ 0.01	0.25 $\pm$ 0.05	0.21 $\pm$ 0.01	0.47 $\pm$ 0.12	0.4 $\pm$ 0.03	0.5 $\pm$ 0.08	0.46 $\pm$ 0.02	0.23 $\pm$ 0.04	0.2 $\pm$ 0.01
	<b>WLS</b>	0.15 $\pm$ 0.03	0.13 $\pm$ 0.01	0.26 $\pm$ 0.06	0.23 $\pm$ 0.01	0.26 $\pm$ 0.06	0.23 $\pm$ 0.02	0.45 $\pm$ 0.13	0.42 $\pm$ 0.03	0.56 $\pm$ 0.08	0.52 $\pm$ 0.03	0.23 $\pm$ 0.03	0.21 $\pm$ 0.01
	<b>wPLS</b>	0.15 $\pm$ 0.03	0.14 $\pm$ 0.01	0.25 $\pm$ 0.06	0.23 $\pm$ 0.01	0.25 $\pm$ 0.05	0.23 $\pm$ 0.02	0.45 $\pm$ 0.12	0.43 $\pm$ 0.03	0.56 $\pm$ 0.08	0.52 $\pm$ 0.03	0.23 $\pm$ 0.03	0.21 $\pm$ 0.01
	<b>PLS</b>	0.14 $\pm$ 0.03	0.12 $\pm$ 0.01	0.25 $\pm$ 0.05	0.23 $\pm$ 0.01	0.24 $\pm$ 0.05	0.21 $\pm$ 0.01	0.45 $\pm$ 0.12	0.4 $\pm$ 0.03	0.49 $\pm$ 0.08	0.46 $\pm$ 0.02	0.23 $\pm$ 0.04	0.2 $\pm$ 0.01
	<b>wRidge</b>	0.15 $\pm$ 0.03	0.13 $\pm$ 0.01	0.26 $\pm$ 0.06	0.23 $\pm$ 0.01	0.26 $\pm$ 0.06	0.23 $\pm$ 0.02	0.45 $\pm$ 0.13	0.42 $\pm$ 0.03	0.56 $\pm$ 0.08	0.52 $\pm$ 0.03	0.23 $\pm$ 0.03	0.21 $\pm$ 0.01
	<b>Ridge</b>	0.15 $\pm$ 0.03	0.12 $\pm$ 0.01	0.26 $\pm$ 0.05	0.23 $\pm$ 0.01	0.25 $\pm$ 0.05	0.21 $\pm$ 0.01	0.47 $\pm$ 0.12	0.4 $\pm$ 0.03	0.5 $\pm$ 0.08	0.46 $\pm$ 0.02	0.23 $\pm$ 0.04	0.2 $\pm$ 0.01
	<b>wLasso</b>	0.14 $\pm$ 0.03	0.13 $\pm$ 0.01	0.25 $\pm$ 0.06	0.23 $\pm$ 0.01	0.27 $\pm$ 0.07	0.25 $\pm$ 0.02	0.46 $\pm$ 0.13	0.44 $\pm$ 0.03	0.56 $\pm$ 0.08	0.52 $\pm$ 0.03	0.23 $\pm$ 0.03	0.21 $\pm$ 0.01
	<b>Lasso</b>	0.14 $\pm$ 0.03	0.12 $\pm$ 0.01	0.25 $\pm$ 0.05	0.23 $\pm$ 0.01	0.24 $\pm$ 0.05	0.21 $\pm$ 0.01	0.47 $\pm$ 0.12	0.4 $\pm$ 0.03	0.5 $\pm$ 0.08	0.46 $\pm$ 0.02	0.23 $\pm$ 0.04	0.2 $\pm$ 0.01
	<b>GLM</b>	0.23 $\pm$ 0.07	0.18 $\pm$ 0.01	0.41 $\pm$ 0.08	0.31 $\pm$ 0.03	0.49 $\pm$ 0.11	0.38 $\pm$ 0.02	0.71 $\pm$ 0.15	0.58 $\pm$ 0.03	0.63 $\pm$ 0.1	0.54 $\pm$ 0.03	0.27 $\pm$ 0.05	0.22 $\pm$ 0.01
	<b>RF</b>	0.18 $\pm$ 0.04	0.07 $\pm$ 0.01	0.27 $\pm$ 0.06	0.11 $\pm$ 0.01	0.33 $\pm$ 0.09	0.13 $\pm$ 0.01	0.52 $\pm$ 0.18	0.2 $\pm$ 0.02	0.59 $\pm$ 0.1	0.23 $\pm$ 0.02	0.24 $\pm$ 0.04	0.09 $\pm$ 0.01
	<b>MLP</b>	0.22 $\pm$ 0.07	0.16 $\pm$ 0.08	0.32 $\pm$ 0.08	0.24 $\pm$ 0.08	0.33 $\pm$ 0.09	0.27 $\pm$ 0.07	0.58 $\pm$ 0.2	0.52 $\pm$ 0.16	0.59 $\pm$ 0.14	0.5 $\pm$ 0.14	0.29 $\pm$ 0.08	0.22 $\pm$ 0.08
DTT	<b>OLS</b>	0.29 $\pm$ 0.05	0.25 $\pm$ 0.01	0.45 $\pm$ 0.09	0.39 $\pm$ 0.03	0.32 $\pm$ 0.05	0.29 $\pm$ 0.01	0.38 $\pm$ 0.09	0.31 $\pm$ 0.02	0.68 $\pm$ 0.09	0.61 $\pm$ 0.02	0.31 $\pm$ 0.05	0.27 $\pm$ 0.02
	<b>WLS</b>	0.32 $\pm$ 0.06	0.28 $\pm$ 0.02	0.47 $\pm$ 0.11	0.41 $\pm$ 0.03	0.43 $\pm$ 0.06	0.38 $\pm$ 0.03	0.36 $\pm$ 0.09	0.31 $\pm$ 0.02	0.7 $\pm$ 0.1	0.65 $\pm$ 0.03	0.32 $\pm$ 0.06	0.28 $\pm$ 0.01
	<b>wPLS</b>	0.32 $\pm$ 0.06	0.27 $\pm$ 0.02	0.43 $\pm$ 0.1	0.39 $\pm$ 0.03	0.45 $\pm$ 0.07	0.42 $\pm$ 0.05	0.36 $\pm$ 0.09	0.31 $\pm$ 0.02	0.69 $\pm$ 0.1	0.65 $\pm$ 0.03	0.32 $\pm$ 0.06	0.28 $\pm$ 0.01
	<b>PLS</b>	0.29 $\pm$ 0.05	0.25 $\pm$ 0.01	0.44 $\pm$ 0.09	0.38 $\pm$ 0.03	0.32 $\pm$ 0.05	0.29 $\pm$ 0.01	0.38 $\pm$ 0.08	0.31 $\pm$ 0.02	0.67 $\pm$ 0.09	0.62 $\pm$ 0.02	0.31 $\pm$ 0.05	0.27 $\pm$ 0.02
	<b>wRidge</b>	0.32 $\pm$ 0.06	0.28 $\pm$ 0.02	0.47 $\pm$ 0.11	0.41 $\pm$ 0.03	0.43 $\pm$ 0.06	0.38 $\pm$ 0.03	0.36 $\pm$ 0.09	0.31 $\pm$ 0.02	0.7 $\pm$ 0.1	0.65 $\pm$ 0.03	0.32 $\pm$ 0.06	0.28 $\pm$ 0.01
	<b>Ridge</b>	0.29 $\pm$ 0.05	0.25 $\pm$ 0.01	0.45 $\pm$ 0.09	0.39 $\pm$ 0.03	0.32 $\pm$ 0.05	0.29 $\pm$ 0.01	0.38 $\pm$ 0.09	0.31 $\pm$ 0.02	0.68 $\pm$ 0.09	0.61 $\pm$ 0.02	0.31 $\pm$ 0.05	0.27 $\pm$ 0.02
	<b>wLasso</b>	0.31 $\pm$ 0.05	0.27 $\pm$ 0.02	0.46 $\pm$ 0.11	0.41 $\pm$ 0.04	0.47 $\pm$ 0.07	0.44 $\pm$ 0.03	0.36 $\pm$ 0.09	0.31 $\pm$ 0.02	0.69 $\pm$ 0.1	0.65 $\pm$ 0.03	0.32 $\pm$ 0.06	0.28 $\pm$ 0.01
	<b>Lasso</b>	0.29 $\pm$ 0.05	0.26 $\pm$ 0.01	0.44 $\pm$ 0.09	0.39 $\pm$ 0.03	0.32 $\pm$ 0.05	0.29 $\pm$ 0.01	0.39 $\pm$ 0.08	0.31 $\pm$ 0.02	0.68 $\pm$ 0.09	0.61 $\pm$ 0.02	0.31 $\pm$ 0.05	0.27 $\pm$ 0.02
	<b>GLM</b>	0.35 $\pm$ 0.06	0.29 $\pm$ 0.01	0.51 $\pm$ 0.11	0.41 $\pm$ 0.03	0.44 $\pm$ 0.1	0.36 $\pm$ 0.02	0.51 $\pm$ 0.12	0.39 $\pm$ 0.03	0.78 $\pm$ 0.12	0.67 $\pm$ 0.03	0.3 $\pm$ 0.06	0.25 $\pm$ 0.01
	<b>RF</b>	0.41 $\pm$ 0.08	0.16 $\pm$ 0.01	0.49 $\pm$ 0.11	0.19 $\pm$ 0.02	0.41 $\pm$ 0.08	0.16 $\pm$ 0.01	0.49 $\pm$ 0.13	0.19 $\pm$ 0.02	0.73 $\pm$ 0.11	0.28 $\pm$ 0.02	0.37 $\pm$ 0.09	0.15 $\pm$ 0.01
	<b>MLP</b>	0.4 $\pm$ 0.12	0.32 $\pm$ 0.09	0.52 $\pm$ 0.14	0.41 $\pm$ 0.11	0.41 $\pm$ 0.1	0.34 $\pm$ 0.08	0.53 $\pm$ 0.18	0.44 $\pm$ 0.18	0.73 $\pm$ 0.14	0.63 $\pm$ 0.12	0.44 $\pm$ 0.13	0.39 $\pm$ 0.12

Table S. 5. RMSE (mean  $\pm$  std ) of the training and testing datasets of all models in  $\text{PM}_{10}\text{OP}_{\text{AA}}$  and  $\text{PM}_{10}\text{OP}_{\text{DTT}}$  prediction

OPtype	Methods	PdBtest	PdBtrain	TALtest	TALtrain	GRE-frtest	GRE-frtrain	CHAMtest	CHAMtrain	RBXtest	RBXtrain	NICtest	NICtrain
<b>AA</b>	<b>OLS</b>	0.21 $\pm$ 0.05	0.18 $\pm$ 0.01	0.38 $\pm$ 0.09	0.33 $\pm$ 0.02	0.36 $\pm$ 0.1	0.31 $\pm$ 0.03	0.73 $\pm$ 0.21	0.63 $\pm$ 0.05	0.71 $\pm$ 0.12	0.64 $\pm$ 0.03	0.29 $\pm$ 0.05	0.25 $\pm$ 0.01
	<b>WLS</b>	0.22 $\pm$ 0.05	0.19 $\pm$ 0.01	0.41 $\pm$ 0.11	0.39 $\pm$ 0.04	0.4 $\pm$ 0.12	0.37 $\pm$ 0.04	0.73 $\pm$ 0.23	0.72 $\pm$ 0.07	0.78 $\pm$ 0.15	0.74 $\pm$ 0.04	0.29 $\pm$ 0.05	0.26 $\pm$ 0.01
	<b>wPLS</b>	0.21 $\pm$ 0.05	0.19 $\pm$ 0.01	0.4 $\pm$ 0.11	0.38 $\pm$ 0.03	0.37 $\pm$ 0.1	0.35 $\pm$ 0.04	0.73 $\pm$ 0.23	0.74 $\pm$ 0.06	0.78 $\pm$ 0.15	0.74 $\pm$ 0.04	0.28 $\pm$ 0.04	0.26 $\pm$ 0.01
	<b>PLS</b>	0.2 $\pm$ 0.05	0.18 $\pm$ 0.01	0.37 $\pm$ 0.09	0.33 $\pm$ 0.02	0.35 $\pm$ 0.1	0.32 $\pm$ 0.03	0.7 $\pm$ 0.21	0.64 $\pm$ 0.05	0.7 $\pm$ 0.12	0.65 $\pm$ 0.03	0.28 $\pm$ 0.04	0.26 $\pm$ 0.01
	<b>wRidge</b>	0.22 $\pm$ 0.05	0.19 $\pm$ 0.01	0.41 $\pm$ 0.11	0.39 $\pm$ 0.04	0.4 $\pm$ 0.12	0.37 $\pm$ 0.04	0.73 $\pm$ 0.23	0.72 $\pm$ 0.07	0.78 $\pm$ 0.15	0.74 $\pm$ 0.04	0.29 $\pm$ 0.05	0.26 $\pm$ 0.01
	<b>Ridge</b>	0.21 $\pm$ 0.05	0.18 $\pm$ 0.01	0.38 $\pm$ 0.09	0.33 $\pm$ 0.02	0.36 $\pm$ 0.1	0.31 $\pm$ 0.03	0.73 $\pm$ 0.21	0.63 $\pm$ 0.05	0.71 $\pm$ 0.12	0.64 $\pm$ 0.03	0.29 $\pm$ 0.05	0.25 $\pm$ 0.01
	<b>wLasso</b>	0.21 $\pm$ 0.06	0.19 $\pm$ 0.01	0.41 $\pm$ 0.11	0.39 $\pm$ 0.04	0.43 $\pm$ 0.12	0.41 $\pm$ 0.03	0.75 $\pm$ 0.24	0.75 $\pm$ 0.07	0.77 $\pm$ 0.15	0.73 $\pm$ 0.04	0.28 $\pm$ 0.04	0.26 $\pm$ 0.01
	<b>Lasso</b>	0.2 $\pm$ 0.05	0.18 $\pm$ 0.01	0.37 $\pm$ 0.09	0.33 $\pm$ 0.02	0.37 $\pm$ 0.1	0.31 $\pm$ 0.03	0.73 $\pm$ 0.21	0.63 $\pm$ 0.05	0.7 $\pm$ 0.12	0.64 $\pm$ 0.03	0.29 $\pm$ 0.04	0.25 $\pm$ 0.01
	<b>GLM</b>	0.34 $\pm$ 0.19	0.23 $\pm$ 0.02	0.61 $\pm$ 0.21	0.4 $\pm$ 0.03	0.71 $\pm$ 0.31	0.48 $\pm$ 0.03	0.93 $\pm$ 0.26	0.74 $\pm$ 0.04	0.94 $\pm$ 0.25	0.72 $\pm$ 0.04	0.37 $\pm$ 0.1	0.27 $\pm$ 0.01
	<b>RF</b>	0.26 $\pm$ 0.06	0.11 $\pm$ 0.01	0.41 $\pm$ 0.14	0.18 $\pm$ 0.03	0.5 $\pm$ 0.16	0.21 $\pm$ 0.03	0.86 $\pm$ 0.36	0.37 $\pm$ 0.06	0.82 $\pm$ 0.17	0.35 $\pm$ 0.03	0.31 $\pm$ 0.05	0.13 $\pm$ 0.01
	<b>MLP</b>	0.3 $\pm$ 0.1	0.2 $\pm$ 0.1	0.45 $\pm$ 0.12	0.33 $\pm$ 0.11	0.48 $\pm$ 0.15	0.39 $\pm$ 0.09	0.86 $\pm$ 0.3	0.79 $\pm$ 0.23	0.81 $\pm$ 0.2	0.69 $\pm$ 0.2	0.36 $\pm$ 0.1	0.28 $\pm$ 0.1
<b>DTT</b>	<b>OLS</b>	0.39 $\pm$ 0.08	0.34 $\pm$ 0.02	0.67 $\pm$ 0.22	0.59 $\pm$ 0.06	0.42 $\pm$ 0.08	0.38 $\pm$ 0.02	0.55 $\pm$ 0.14	0.44 $\pm$ 0.03	0.89 $\pm$ 0.14	0.78 $\pm$ 0.03	0.39 $\pm$ 0.07	0.34 $\pm$ 0.02
	<b>WLS</b>	0.42 $\pm$ 0.09	0.37 $\pm$ 0.02	0.71 $\pm$ 0.23	0.66 $\pm$ 0.06	0.54 $\pm$ 0.09	0.5 $\pm$ 0.03	0.53 $\pm$ 0.16	0.47 $\pm$ 0.04	0.94 $\pm$ 0.17	0.9 $\pm$ 0.05	0.41 $\pm$ 0.07	0.37 $\pm$ 0.02
	<b>wPLS</b>	0.42 $\pm$ 0.09	0.37 $\pm$ 0.02	0.66 $\pm$ 0.21	0.63 $\pm$ 0.06	0.57 $\pm$ 0.09	0.54 $\pm$ 0.06	0.53 $\pm$ 0.16	0.47 $\pm$ 0.04	0.92 $\pm$ 0.17	0.89 $\pm$ 0.05	0.41 $\pm$ 0.07	0.37 $\pm$ 0.02
	<b>PLS</b>	0.39 $\pm$ 0.08	0.34 $\pm$ 0.02	0.66 $\pm$ 0.22	0.59 $\pm$ 0.06	0.42 $\pm$ 0.08	0.38 $\pm$ 0.02	0.55 $\pm$ 0.13	0.44 $\pm$ 0.03	0.88 $\pm$ 0.14	0.8 $\pm$ 0.03	0.39 $\pm$ 0.07	0.34 $\pm$ 0.02
	<b>wRidge</b>	0.42 $\pm$ 0.09	0.37 $\pm$ 0.02	0.71 $\pm$ 0.23	0.66 $\pm$ 0.06	0.54 $\pm$ 0.09	0.5 $\pm$ 0.03	0.53 $\pm$ 0.16	0.47 $\pm$ 0.04	0.94 $\pm$ 0.17	0.9 $\pm$ 0.05	0.41 $\pm$ 0.07	0.37 $\pm$ 0.02
	<b>Ridge</b>	0.39 $\pm$ 0.08	0.34 $\pm$ 0.02	0.67 $\pm$ 0.22	0.59 $\pm$ 0.06	0.42 $\pm$ 0.08	0.38 $\pm$ 0.02	0.55 $\pm$ 0.14	0.44 $\pm$ 0.03	0.89 $\pm$ 0.14	0.78 $\pm$ 0.03	0.39 $\pm$ 0.07	0.34 $\pm$ 0.02
	<b>wLasso</b>	0.42 $\pm$ 0.08	0.37 $\pm$ 0.02	0.7 $\pm$ 0.23	0.65 $\pm$ 0.06	0.59 $\pm$ 0.1	0.57 $\pm$ 0.04	0.54 $\pm$ 0.17	0.49 $\pm$ 0.04	0.93 $\pm$ 0.17	0.89 $\pm$ 0.05	0.41 $\pm$ 0.07	0.38 $\pm$ 0.02
	<b>Lasso</b>	0.39 $\pm$ 0.08	0.34 $\pm$ 0.02	0.67 $\pm$ 0.22	0.59 $\pm$ 0.06	0.41 $\pm$ 0.08	0.38 $\pm$ 0.02	0.56 $\pm$ 0.13	0.44 $\pm$ 0.03	0.88 $\pm$ 0.14	0.78 $\pm$ 0.03	0.39 $\pm$ 0.07	0.34 $\pm$ 0.02
	<b>GLM</b>	0.45 $\pm$ 0.09	0.36 $\pm$ 0.02	0.78 $\pm$ 0.23	0.6 $\pm$ 0.05	0.58 $\pm$ 0.21	0.45 $\pm$ 0.02	0.71 $\pm$ 0.25	0.5 $\pm$ 0.03	1.1 $\pm$ 0.31	0.86 $\pm$ 0.05	0.4 $\pm$ 0.08	0.32 $\pm$ 0.02
	<b>RF</b>	0.54 $\pm$ 0.12	0.22 $\pm$ 0.02	0.74 $\pm$ 0.21	0.31 $\pm$ 0.04	0.54 $\pm$ 0.11	0.23 $\pm$ 0.02	0.71 $\pm$ 0.21	0.29 $\pm$ 0.03	0.95 $\pm$ 0.18	0.39 $\pm$ 0.03	0.51 $\pm$ 0.13	0.21 $\pm$ 0.02
	<b>MLP</b>	0.52 $\pm$ 0.15	0.41 $\pm$ 0.12	0.78 $\pm$ 0.23	0.6 $\pm$ 0.15	0.53 $\pm$ 0.15	0.44 $\pm$ 0.11	0.74 $\pm$ 0.26	0.6 $\pm$ 0.26	0.97 $\pm$ 0.25	0.83 $\pm$ 0.2	0.56 $\pm$ 0.17	0.5 $\pm$ 0.16

Variations of the intrinsic  $\text{OP}_{\text{AA}}$  values of the different PM sources among different models.

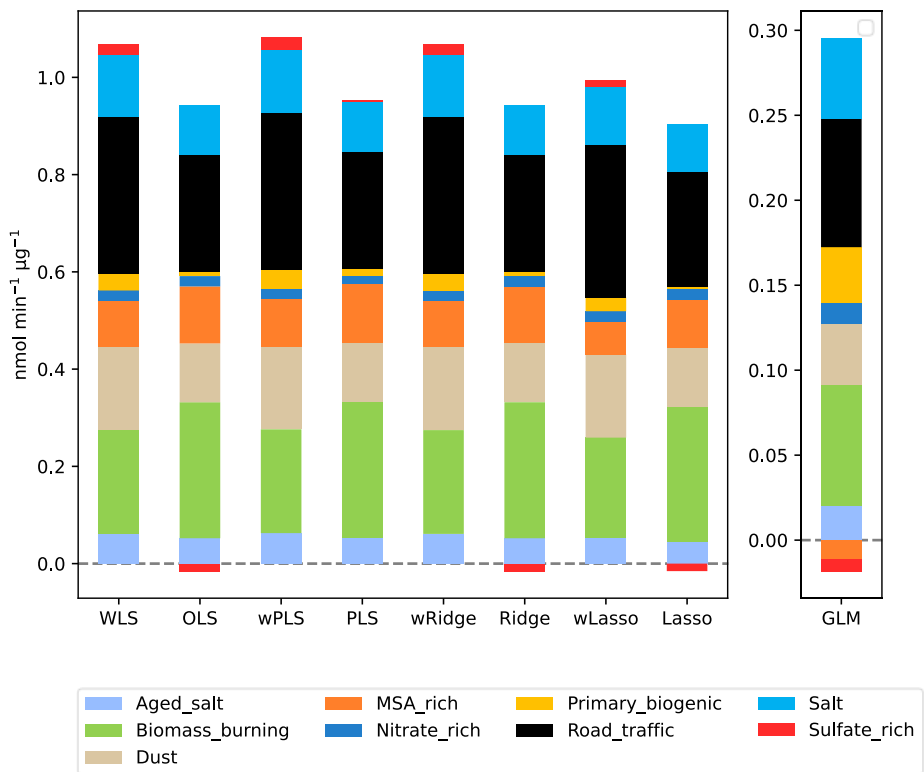


Figure S. 3. Variations of intrinsic  $\text{PM}_{10}\text{OP}_{\text{AA}}$  by model in RBX

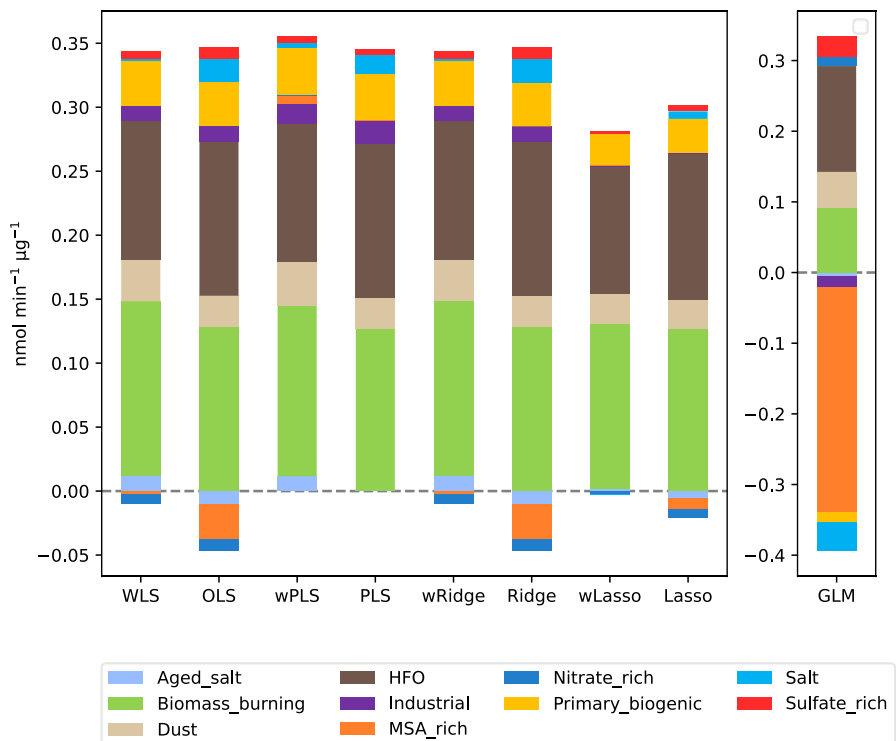
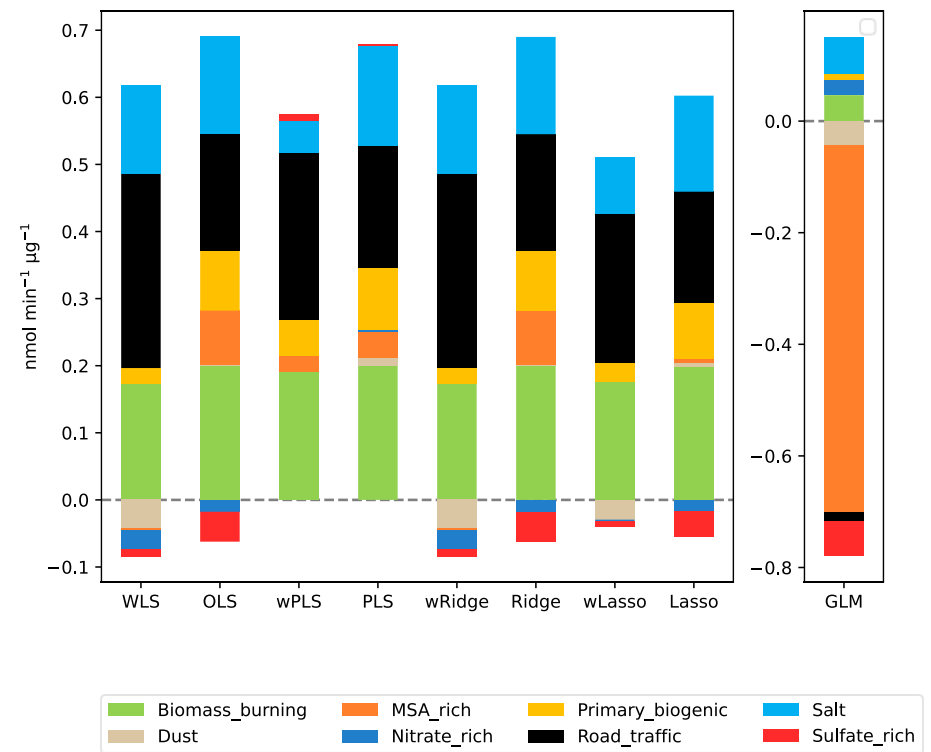
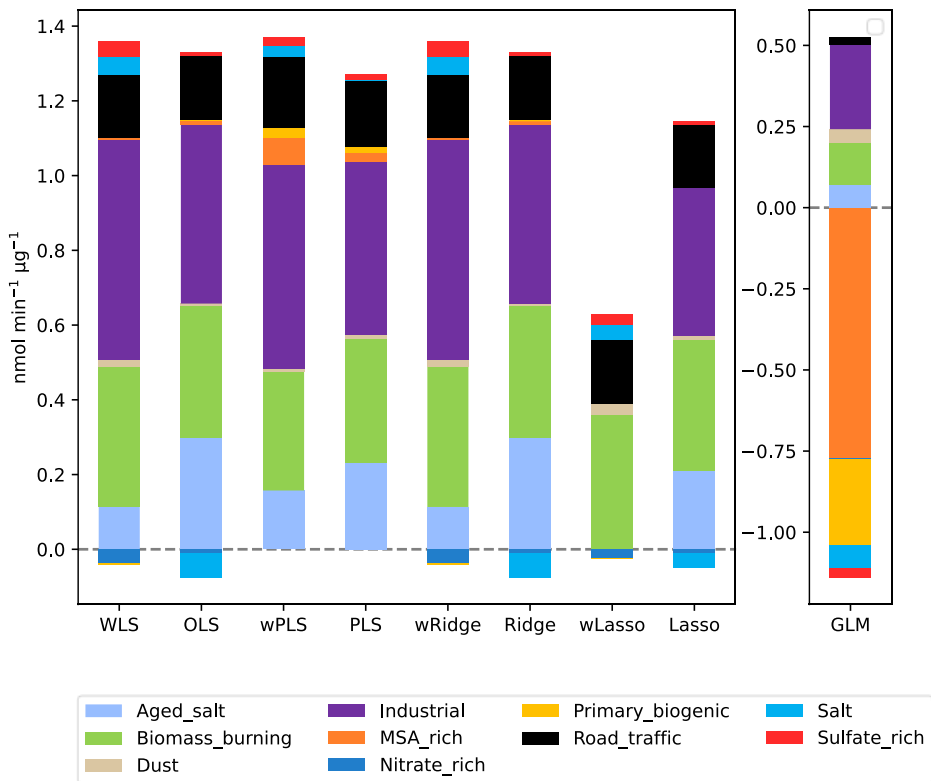
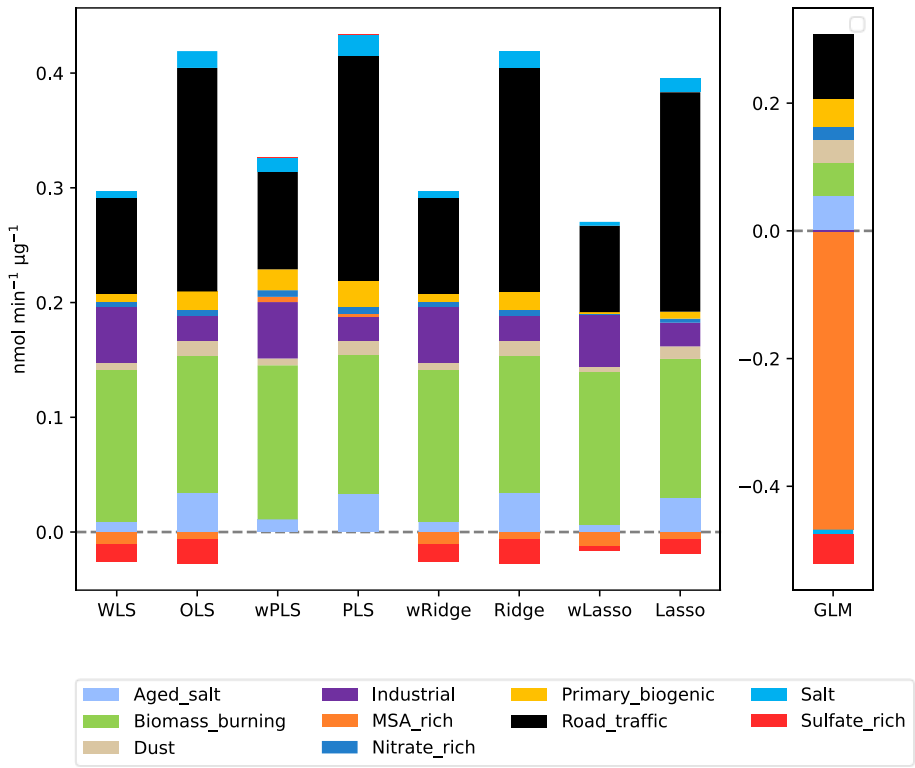
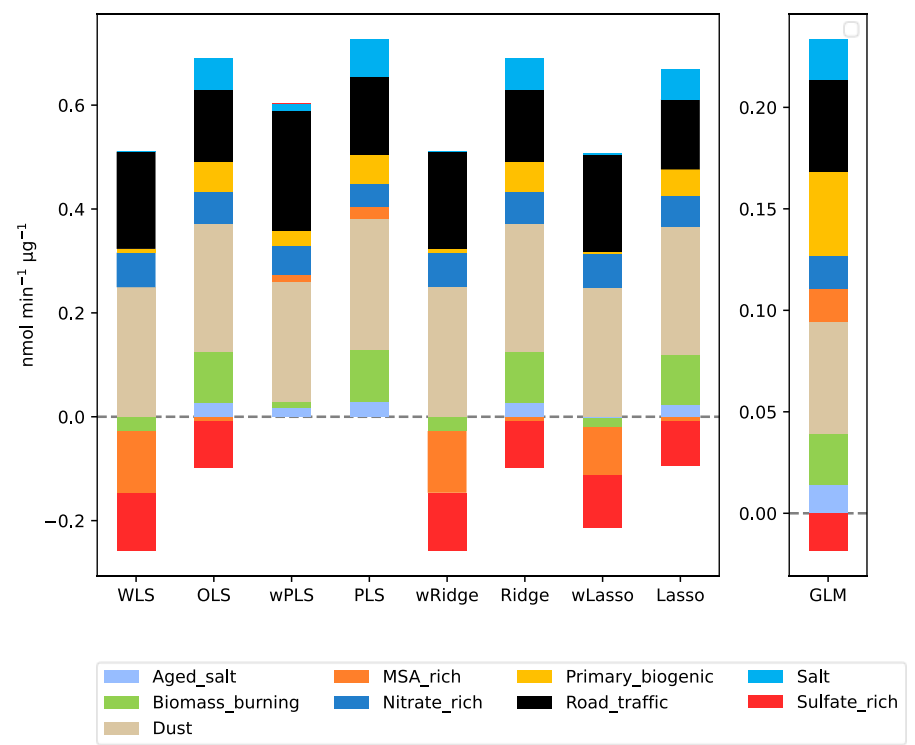


Figure S. 4. Variations of intrinsic  $\text{PM}_{10}\text{OP}_{\text{AA}}$  by model in PdB





### S7. Variations of the intrinsic OP<sub>DTT</sub> values of the different PM sources among different models.



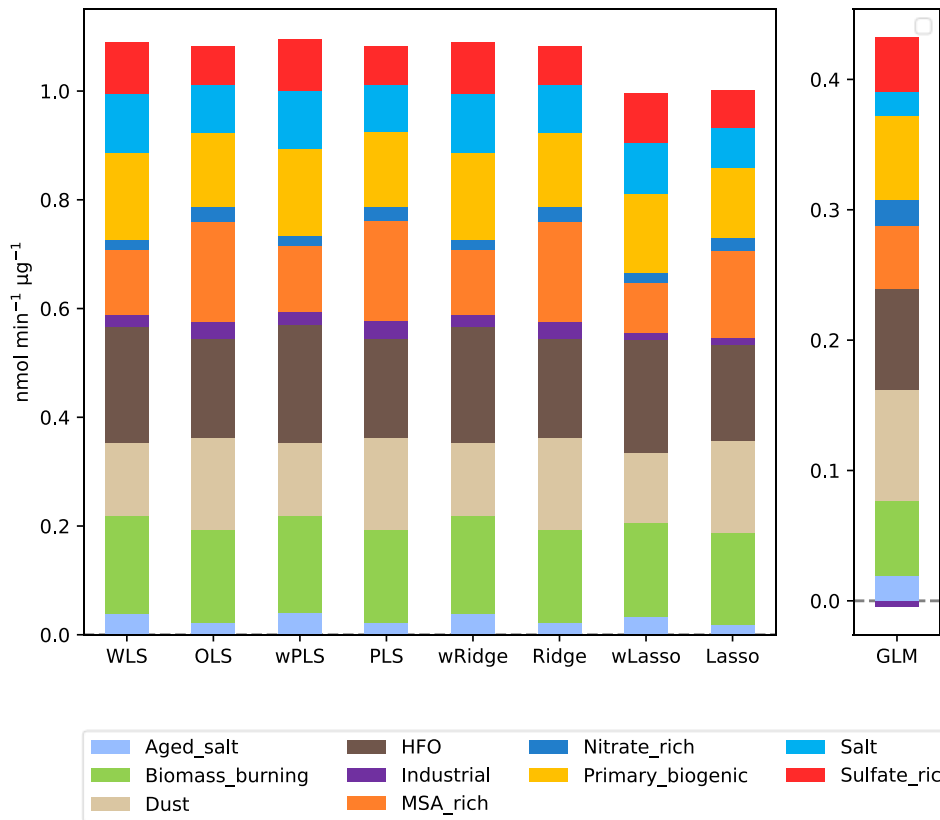


Figure S. 9. Variations of intrinsic PM<sub>10</sub> OP<sub>DTT</sub> by model in PdB

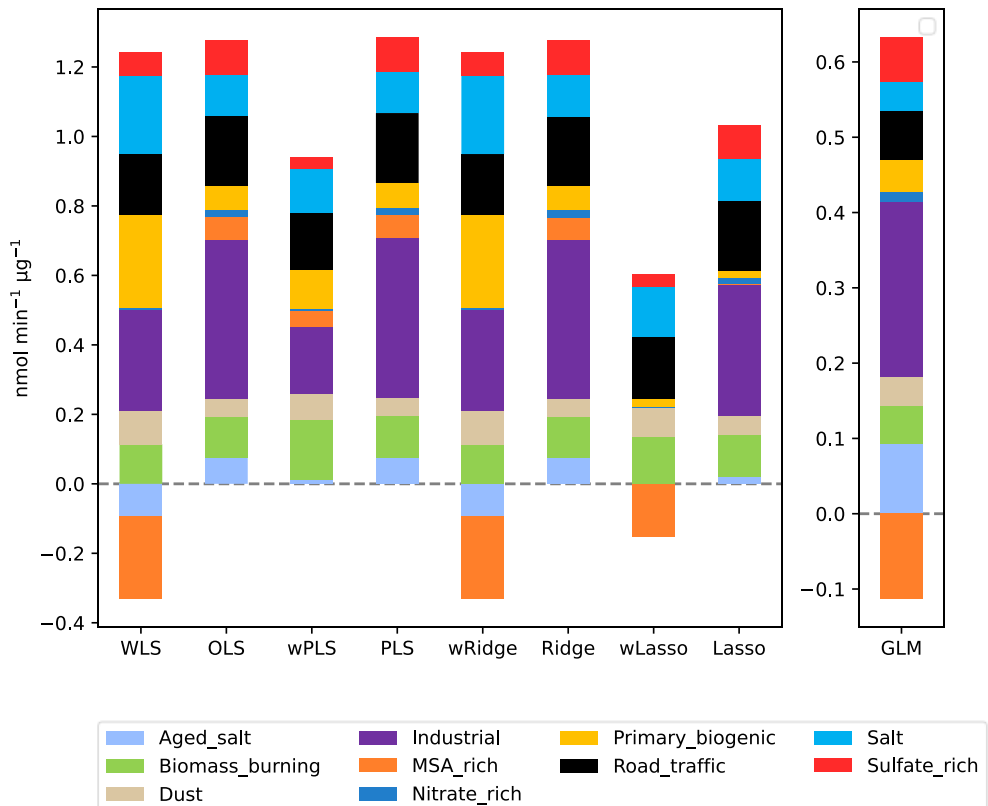


Figure S. 10. Variations of intrinsic PM<sub>10</sub> OP<sub>DTT</sub> by model in GRE-fr

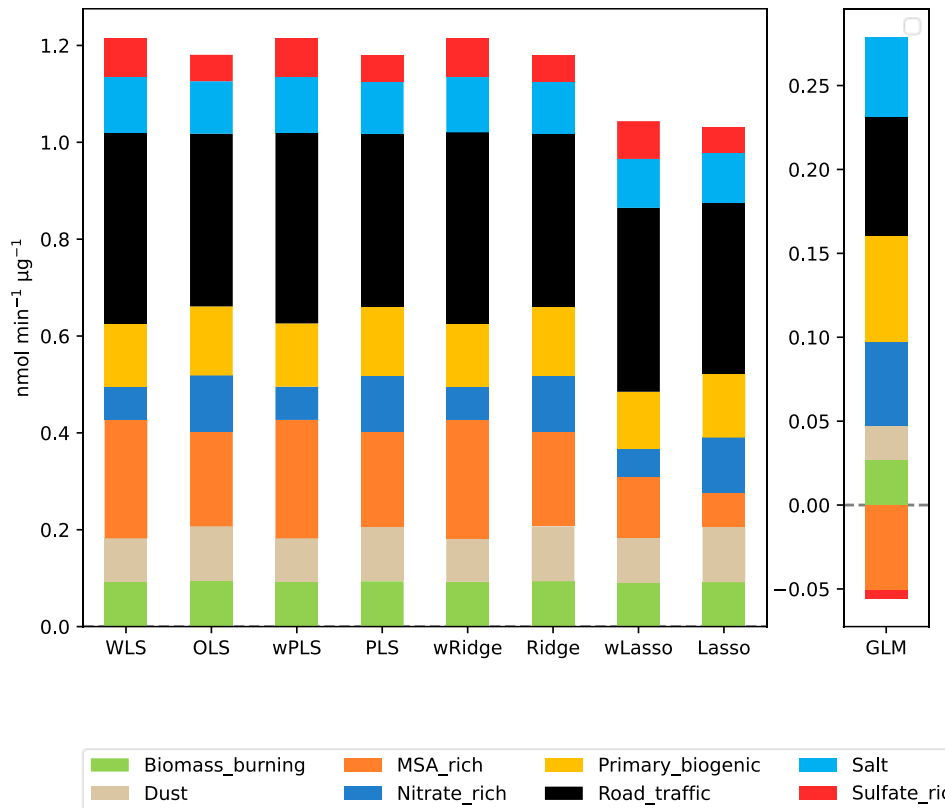


Figure S. 11. Variations of intrinsic PM<sub>10</sub> OP<sub>DTT</sub> by model in CHAM

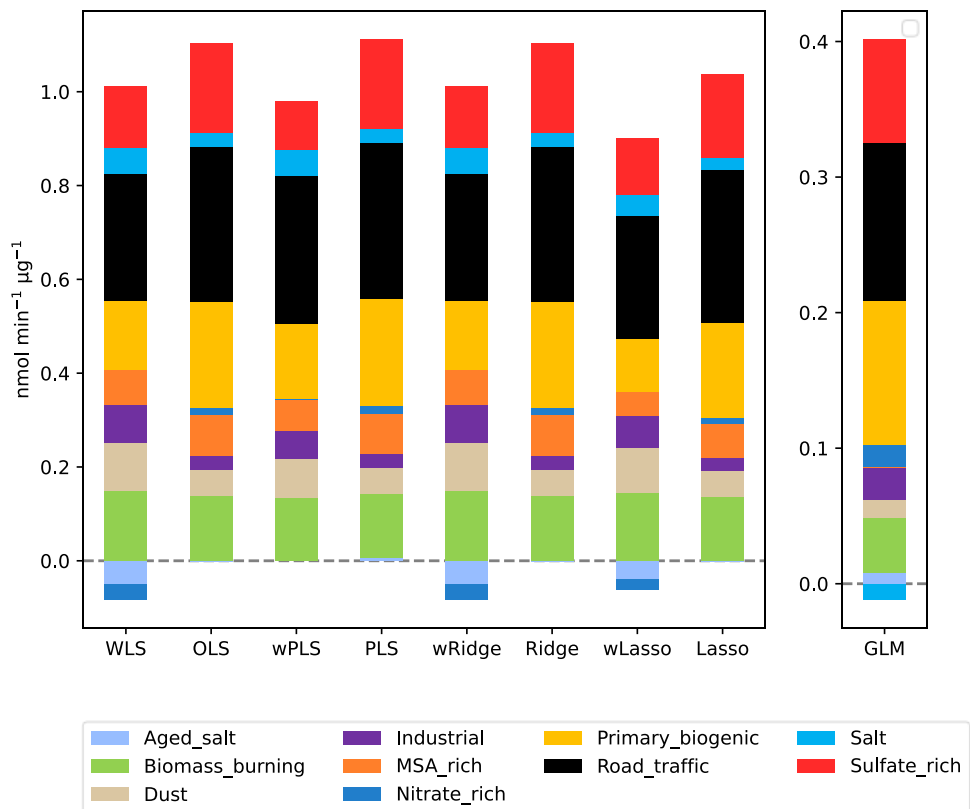


Figure S. 12. Variations of intrinsic PM<sub>10</sub> OP<sub>DTT</sub> by model in TAL

Table S. 6. Intrinsic PM<sub>10</sub>OP<sub>AA</sub> (mean ± std) of all models (in nmol min<sup>-1</sup> µg<sup>-1</sup>)

Site	Method	Aged salt	Biomass burning	Dust	HFO	Industrial	MSA rich	Nitrate rich	Primary biogenic	Salt	Sulfate rich	Road traffic
PdB	<b>OLS</b>	-0.01±0.01	0.13±0.0	0.02±0.0	0.12±0.01	0.01±0.01	-0.03±0.01	-0.01±0.01	0.03±0.01	0.02±0.01	0.01±0.01	
	<b>WLS</b>	0.01±0.01	0.14±0.01	0.03±0.01	0.11±0.02	0.01±0.01	-0.0±0.02	-0.01±0.01	0.03±0.01	0.0±0.01	0.01±0.01	
	<b>wPLS</b>	0.01±0.01	0.13±0.01	0.03±0.01	0.11±0.02	0.02±0.01	0.01±0.01	0.0±0.0	0.04±0.01	0.0±0.01	0.0±0.0	
	<b>PLS</b>	0.0±0.0	0.13±0.0	0.02±0.01	0.12±0.01	0.02±0.01	0.0±0.0	0.0±0.0	0.04±0.01	0.01±0.01	0.0±0.0	
	<b>wRidge</b>	0.01±0.01	0.14±0.01	0.03±0.01	0.11±0.02	0.01±0.01	-0.0±0.02	-0.01±0.01	0.03±0.01	0.0±0.01	0.01±0.01	
	<b>Ridge</b>	-0.01±0.01	0.13±0.0	0.02±0.0	0.12±0.01	0.01±0.01	-0.03±0.01	-0.01±0.01	0.03±0.01	0.02±0.01	0.01±0.01	
	<b>wLasso</b>	0.0±0.0	0.13±0.0	0.02±0.01	0.1±0.02	0.0±0.0	0.0±0.0	-0.0±0.01	0.02±0.01	-0.0±0.0	0.0±0.0	
	<b>Lasso</b>	-0.01±0.01	0.13±0.0	0.02±0.0	0.11±0.01	0.0±0.0	-0.01±0.01	-0.01±0.0	0.03±0.01	0.01±0.01	0.0±0.0	
	<b>GLM</b>	-0.01±0.02	0.09±0.01	0.05±0.02	0.15±0.03	-0.02±0.05	-0.32±0.08	0.01±0.01	-0.01±0.02	-0.04±0.03	0.03±0.01	
TAL	<b>OLS</b>	0.03±0.01	0.12±0.01	0.01±0.01		0.02±0.02	-0.01±0.02	0.0±0.01	0.02±0.02	0.01±0.01	-0.02±0.02	0.19±0.03
	<b>WLS</b>	0.01±0.01	0.13±0.01	0.01±0.01		0.05±0.02	-0.01±0.03	0.0±0.01	0.01±0.02	0.01±0.01	-0.02±0.02	0.08±0.04
	<b>wPLS</b>	0.01±0.01	0.13±0.01	0.01±0.01		0.05±0.02	0.0±0.01	0.01±0.0	0.02±0.01	0.01±0.01	0.0±0.0	0.09±0.04
	<b>PLS</b>	0.03±0.01	0.12±0.01	0.01±0.01		0.02±0.02	0.0±0.01	0.01±0.0	0.02±0.02	0.02±0.01	0.0±0.0	0.2±0.03
	<b>wRidge</b>	0.01±0.01	0.13±0.01	0.01±0.01		0.05±0.02	-0.01±0.03	0.0±0.01	0.01±0.02	0.01±0.01	-0.02±0.02	0.08±0.04
	<b>Ridge</b>	0.03±0.01	0.12±0.01	0.01±0.01		0.02±0.02	-0.01±0.02	0.0±0.01	0.02±0.02	0.01±0.01	-0.02±0.02	0.19±0.03
	<b>wLasso</b>	0.01±0.01	0.13±0.01	0.0±0.01		0.04±0.02	-0.01±0.01	0.0±0.0	0.0±0.01	0.0±0.0	-0.0±0.01	0.08±0.04
	<b>Lasso</b>	0.03±0.01	0.12±0.01	0.01±0.01		0.02±0.02	-0.01±0.01	0.0±0.0	0.01±0.01	0.01±0.01	-0.01±0.01	0.19±0.03
	<b>GLM</b>	0.06±0.02	0.05±0.01	0.04±0.02		-0.0±0.03	-0.47±0.11	0.02±0.01	0.04±0.05	-0.01±0.02	-0.05±0.04	0.1±0.04
GRE-fr	<b>OLS</b>	0.3±0.07	0.35±0.01	0.01±0.01		0.48±0.08	0.01±0.06	-0.01±0.01	0.0±0.03	-0.07±0.04	0.01±0.01	0.17±0.01
	<b>WLS</b>	0.11±0.07	0.38±0.02	0.02±0.01		0.59±0.13	0.01±0.07	-0.04±0.02	-0.0±0.03	0.05±0.04	0.04±0.01	0.17±0.02
	<b>wPLS</b>	0.16±0.07	0.32±0.03	0.01±0.01		0.54±0.14	0.07±0.06	0.0±0.0	0.03±0.02	0.03±0.04	0.02±0.01	0.19±0.02
	<b>PLS</b>	0.23±0.04	0.33±0.01	0.01±0.01		0.46±0.08	0.02±0.03	0.0±0.0	0.02±0.02	0.0±0.01	0.01±0.01	0.18±0.01
	<b>wRidge</b>	0.11±0.07	0.38±0.02	0.02±0.01		0.59±0.13	0.01±0.07	-0.04±0.02	-0.0±0.03	0.05±0.04	0.04±0.01	0.17±0.02
	<b>Ridge</b>	0.3±0.07	0.35±0.01	0.01±0.01		0.48±0.08	0.01±0.06	-0.01±0.01	0.0±0.03	-0.06±0.04	0.01±0.01	0.17±0.01
	<b>wLasso</b>	0.0±0.0	0.36±0.02	0.03±0.01		0.0±0.0	0.0±0.0	-0.02±0.02	-0.0±0.0	0.04±0.03	0.03±0.01	0.17±0.02
	<b>Lasso</b>	0.21±0.06	0.35±0.01	0.01±0.01		0.4±0.1	0.0±0.0	-0.01±0.01	-0.0±0.01	-0.04±0.03	0.01±0.01	0.17±0.01
	<b>GLM</b>	0.07±0.09	0.13±0.01	0.04±0.02		0.26±0.03	-0.77±0.3	-0.0±0.01	-0.27±0.11	-0.07±0.03	-0.03±0.02	0.02±0.01

Site	Method	Aged salt	Biomass burning	Dust	HFO	Industrial	MSA rich	Nitrate rich	Primary biogenic	Salt	Sulfate rich	Road traffic
CHAM	<b>OLS</b>		0.2±0.01	0.0±0.03		0.08±0.08	-0.02±0.03	0.09±0.03	0.14±0.03	-0.04±0.03	0.17±0.07	
	<b>WLS</b>		0.17±0.01	-0.04±0.01		-0.0±0.03	-0.03±0.03	0.02±0.01	0.13±0.02	-0.01±0.01	0.29±0.03	
	<b>wPLS</b>		0.19±0.01	0.0±0.0		0.02±0.02	0.0±0.0	0.05±0.01	0.05±0.03	0.01±0.01	0.25±0.03	
	<b>PLS</b>		0.2±0.01	0.01±0.02		0.04±0.05	0.0±0.01	0.09±0.02	0.15±0.03	0.0±0.01	0.18±0.07	
	<b>wRidge</b>		0.17±0.01	-0.04±0.01		-0.0±0.03	-0.03±0.03	0.02±0.01	0.13±0.02	-0.01±0.01	0.29±0.03	
	<b>Ridge</b>		0.2±0.01	0.0±0.03		0.08±0.07	-0.02±0.03	0.09±0.03	0.14±0.03	-0.04±0.03	0.17±0.07	
	<b>wLasso</b>		0.18±0.01	-0.03±0.01		0.0±0.0	-0.0±0.01	0.03±0.01	0.08±0.02	-0.01±0.01	0.22±0.03	
	<b>Lasso</b>		0.2±0.01	0.0±0.02		0.01±0.02	-0.02±0.03	0.08±0.03	0.14±0.03	-0.04±0.02	0.17±0.07	
	<b>GLM</b>		0.05±0.0	-0.04±0.02		-0.66±0.14	0.03±0.01	0.01±0.02	0.07±0.01	-0.06±0.02	-0.02±0.04	
RBX	<b>OLS</b>	0.05±0.01	0.28±0.02	0.12±0.01		0.12±0.03	0.02±0.0	0.01±0.02	0.1±0.02	-0.02±0.02	0.24±0.03	
	<b>WLS</b>	0.06±0.02	0.21±0.03	0.17±0.02		0.1±0.05	0.02±0.01	0.03±0.03	0.13±0.02	0.02±0.03	0.32±0.03	
	<b>wPLS</b>	0.06±0.02	0.21±0.03	0.17±0.02		0.1±0.05	0.02±0.01	0.04±0.02	0.13±0.02	0.02±0.02	0.32±0.03	
	<b>PLS</b>	0.05±0.01	0.28±0.02	0.12±0.01		0.12±0.03	0.02±0.0	0.01±0.01	0.1±0.02	0.0±0.01	0.24±0.03	
	<b>wRidge</b>	0.06±0.02	0.21±0.03	0.17±0.02		0.1±0.05	0.02±0.01	0.03±0.03	0.13±0.02	0.02±0.03	0.32±0.03	
	<b>Ridge</b>	0.05±0.01	0.28±0.02	0.12±0.01		0.12±0.03	0.02±0.0	0.01±0.02	0.1±0.02	-0.02±0.02	0.24±0.03	
	<b>wLasso</b>	0.05±0.02	0.21±0.03	0.17±0.02		0.07±0.05	0.02±0.01	0.03±0.03	0.12±0.02	0.01±0.02	0.31±0.03	
	<b>Lasso</b>	0.05±0.01	0.28±0.02	0.12±0.01		0.1±0.03	0.02±0.0	0.01±0.02	0.1±0.02	-0.02±0.02	0.24±0.02	
	<b>GLM</b>	0.02±0.01	0.07±0.01	0.04±0.01		-0.01±0.02	0.01±0.0	0.03±0.02	0.05±0.01	-0.01±0.01	0.08±0.01	
NIC	<b>OLS</b>	0.04±0.01	0.11±0.01	-0.01±0.01		-0.0±0.01	-0.02±0.01	-0.03±0.02	0.04±0.02	0.01±0.01	0.35±0.04	
	<b>WLS</b>	0.03±0.02	0.11±0.01	0.0±0.01		-0.01±0.02	-0.01±0.01	-0.03±0.02	0.05±0.02	0.01±0.01	0.35±0.04	
	<b>wPLS</b>	0.02±0.01	0.12±0.01	0.0±0.0		0.0±0.01	0.0±0.01	0.0±0.0	0.06±0.02	0.01±0.01	0.34±0.03	
	<b>PLS</b>	0.03±0.01	0.11±0.01	0.0±0.0		0.01±0.01	0.0±0.0	0.0±0.0	0.05±0.02	0.01±0.01	0.32±0.03	
	<b>wRidge</b>	0.03±0.02	0.11±0.01	0.0±0.01		-0.01±0.02	-0.01±0.01	-0.03±0.02	0.05±0.02	0.01±0.01	0.35±0.04	
	<b>Ridge</b>	0.04±0.01	0.11±0.01	-0.01±0.01		-0.0±0.01	-0.02±0.01	-0.03±0.02	0.04±0.02	0.01±0.01	0.35±0.04	
	<b>wLasso</b>	0.02±0.01	0.12±0.01	0.0±0.01		0.0±0.01	-0.0±0.0	-0.01±0.01	0.02±0.01	0.0±0.01	0.29±0.03	
	<b>Lasso</b>	0.03±0.01	0.11±0.01	-0.0±0.01		0.0±0.01	-0.01±0.01	-0.02±0.01	0.03±0.02	0.01±0.01	0.31±0.03	
	<b>GLM</b>	0.04±0.02	0.07±0.01	0.01±0.01		-0.04±0.02	-0.02±0.03	-0.03±0.03	0.03±0.03	0.0±0.01	0.32±0.05	

Table S. 7. Intrinsic PM<sub>10</sub> OP<sub>DTT</sub> (mean  $\pm$  std) of all models (in nmol min<sup>-1</sup>  $\mu\text{g}^{-1}$ )

Site	Method	Aged salt	Biomass burning	Dust	HFO	Industrial	MSA rich	Nitrate rich	Primary biogenic	Salt	Sulfate rich	Road traffic
PdB	<b>OLS</b>	0.02 $\pm$ 0.02	0.17 $\pm$ 0.01	0.17 $\pm$ 0.01	0.18 $\pm$ 0.01	0.03 $\pm$ 0.02	0.18 $\pm$ 0.03	0.03 $\pm$ 0.01	0.14 $\pm$ 0.01	0.09 $\pm$ 0.02	0.07 $\pm$ 0.01	
	<b>WLS</b>	0.04 $\pm$ 0.02	0.18 $\pm$ 0.01	0.14 $\pm$ 0.02	0.21 $\pm$ 0.03	0.02 $\pm$ 0.03	0.12 $\pm$ 0.07	0.02 $\pm$ 0.02	0.16 $\pm$ 0.02	0.11 $\pm$ 0.02	0.1 $\pm$ 0.03	
	<b>wPLS</b>	0.04 $\pm$ 0.02	0.18 $\pm$ 0.01	0.14 $\pm$ 0.02	0.22 $\pm$ 0.03	0.03 $\pm$ 0.02	0.12 $\pm$ 0.06	0.02 $\pm$ 0.02	0.16 $\pm$ 0.02	0.11 $\pm$ 0.02	0.1 $\pm$ 0.03	
	<b>PLS</b>	0.02 $\pm$ 0.02	0.17 $\pm$ 0.01	0.17 $\pm$ 0.01	0.18 $\pm$ 0.01	0.03 $\pm$ 0.02	0.18 $\pm$ 0.03	0.03 $\pm$ 0.01	0.14 $\pm$ 0.01	0.09 $\pm$ 0.02	0.07 $\pm$ 0.01	
	<b>wRidge</b>	0.04 $\pm$ 0.02	0.18 $\pm$ 0.01	0.14 $\pm$ 0.02	0.21 $\pm$ 0.03	0.02 $\pm$ 0.03	0.12 $\pm$ 0.07	0.02 $\pm$ 0.02	0.16 $\pm$ 0.02	0.11 $\pm$ 0.02	0.1 $\pm$ 0.03	
	<b>Ridge</b>	0.02 $\pm$ 0.02	0.17 $\pm$ 0.01	0.17 $\pm$ 0.01	0.18 $\pm$ 0.01	0.03 $\pm$ 0.02	0.18 $\pm$ 0.03	0.03 $\pm$ 0.01	0.14 $\pm$ 0.01	0.09 $\pm$ 0.02	0.07 $\pm$ 0.01	
	<b>wLasso</b>	0.03 $\pm$ 0.02	0.17 $\pm$ 0.01	0.13 $\pm$ 0.02	0.21 $\pm$ 0.03	0.01 $\pm$ 0.02	0.09 $\pm$ 0.06	0.02 $\pm$ 0.02	0.15 $\pm$ 0.02	0.09 $\pm$ 0.02	0.09 $\pm$ 0.03	
	<b>Lasso</b>	0.02 $\pm$ 0.02	0.17 $\pm$ 0.01	0.17 $\pm$ 0.01	0.18 $\pm$ 0.01	0.01 $\pm$ 0.01	0.16 $\pm$ 0.03	0.02 $\pm$ 0.01	0.13 $\pm$ 0.01	0.07 $\pm$ 0.02	0.07 $\pm$ 0.01	
	<b>GLM</b>	0.02 $\pm$ 0.01	0.06 $\pm$ 0.01	0.09 $\pm$ 0.01	0.08 $\pm$ 0.01	-0.0 $\pm$ 0.02	0.05 $\pm$ 0.02	0.02 $\pm$ 0.0	0.06 $\pm$ 0.01	0.02 $\pm$ 0.02	0.04 $\pm$ 0.01	
TAL	<b>OLS</b>	-0.0 $\pm$ 0.02	0.14 $\pm$ 0.01	0.06 $\pm$ 0.02		0.03 $\pm$ 0.03	0.09 $\pm$ 0.03	0.02 $\pm$ 0.01	0.23 $\pm$ 0.04	0.03 $\pm$ 0.01	0.19 $\pm$ 0.04	0.33 $\pm$ 0.06
	<b>WLS</b>	-0.05 $\pm$ 0.02	0.15 $\pm$ 0.01	0.1 $\pm$ 0.02		0.08 $\pm$ 0.04	0.08 $\pm$ 0.03	-0.03 $\pm$ 0.02	0.15 $\pm$ 0.03	0.05 $\pm$ 0.02	0.13 $\pm$ 0.04	0.27 $\pm$ 0.07
	<b>wPLS</b>	0.0 $\pm$ 0.0	0.13 $\pm$ 0.01	0.08 $\pm$ 0.02		0.06 $\pm$ 0.04	0.07 $\pm$ 0.03	0.0 $\pm$ 0.0	0.16 $\pm$ 0.03	0.06 $\pm$ 0.02	0.1 $\pm$ 0.04	0.31 $\pm$ 0.06
	<b>PLS</b>	0.01 $\pm$ 0.01	0.14 $\pm$ 0.01	0.06 $\pm$ 0.02		0.03 $\pm$ 0.03	0.09 $\pm$ 0.03	0.02 $\pm$ 0.01	0.23 $\pm$ 0.04	0.03 $\pm$ 0.01	0.19 $\pm$ 0.04	0.33 $\pm$ 0.05
	<b>wRidge</b>	-0.05 $\pm$ 0.02	0.15 $\pm$ 0.01	0.1 $\pm$ 0.02		0.08 $\pm$ 0.04	0.08 $\pm$ 0.03	-0.03 $\pm$ 0.02	0.15 $\pm$ 0.03	0.05 $\pm$ 0.02	0.13 $\pm$ 0.04	0.27 $\pm$ 0.07
	<b>Ridge</b>	-0.0 $\pm$ 0.02	0.14 $\pm$ 0.01	0.06 $\pm$ 0.02		0.03 $\pm$ 0.03	0.09 $\pm$ 0.03	0.02 $\pm$ 0.01	0.23 $\pm$ 0.04	0.03 $\pm$ 0.01	0.19 $\pm$ 0.04	0.33 $\pm$ 0.06
	<b>wLasso</b>	-0.04 $\pm$ 0.02	0.15 $\pm$ 0.01	0.09 $\pm$ 0.02		0.07 $\pm$ 0.03	0.05 $\pm$ 0.03	-0.02 $\pm$ 0.02	0.11 $\pm$ 0.03	0.05 $\pm$ 0.02	0.12 $\pm$ 0.04	0.26 $\pm$ 0.07
	<b>Lasso</b>	-0.0 $\pm$ 0.02	0.14 $\pm$ 0.01	0.06 $\pm$ 0.02		0.03 $\pm$ 0.03	0.07 $\pm$ 0.03	0.01 $\pm$ 0.01	0.2 $\pm$ 0.04	0.02 $\pm$ 0.01	0.18 $\pm$ 0.04	0.33 $\pm$ 0.05
	<b>GLM</b>	0.01 $\pm$ 0.01	0.04 $\pm$ 0.01	0.01 $\pm$ 0.01		0.02 $\pm$ 0.02	0.0 $\pm$ 0.04	0.02 $\pm$ 0.0	0.11 $\pm$ 0.03	-0.01 $\pm$ 0.01	0.08 $\pm$ 0.03	0.12 $\pm$ 0.02
GRE-fr	<b>OLS</b>	0.07 $\pm$ 0.06	0.12 $\pm$ 0.01	0.05 $\pm$ 0.01		0.46 $\pm$ 0.06	0.06 $\pm$ 0.08	0.02 $\pm$ 0.01	0.07 $\pm$ 0.04	0.12 $\pm$ 0.02	0.1 $\pm$ 0.01	0.2 $\pm$ 0.01
	<b>WLS</b>	-0.1 $\pm$ 0.13	0.11 $\pm$ 0.04	0.1 $\pm$ 0.04		0.29 $\pm$ 0.22	-0.24 $\pm$ 0.28	0.0 $\pm$ 0.01	0.27 $\pm$ 0.1	0.23 $\pm$ 0.09	0.07 $\pm$ 0.03	0.17 $\pm$ 0.03
	<b>wPLS</b>	0.01 $\pm$ 0.03	0.17 $\pm$ 0.07	0.08 $\pm$ 0.03		0.19 $\pm$ 0.25	0.05 $\pm$ 0.09	0.01 $\pm$ 0.01	0.11 $\pm$ 0.09	0.12 $\pm$ 0.07	0.03 $\pm$ 0.03	0.16 $\pm$ 0.04
	<b>PLS</b>	0.08 $\pm$ 0.05	0.12 $\pm$ 0.01	0.05 $\pm$ 0.01		0.46 $\pm$ 0.06	0.07 $\pm$ 0.08	0.02 $\pm$ 0.01	0.07 $\pm$ 0.03	0.12 $\pm$ 0.02	0.1 $\pm$ 0.01	0.2 $\pm$ 0.01
	<b>wRidge</b>	-0.1 $\pm$ 0.13	0.11 $\pm$ 0.04	0.1 $\pm$ 0.04		0.29 $\pm$ 0.22	-0.24 $\pm$ 0.28	0.0 $\pm$ 0.01	0.27 $\pm$ 0.1	0.23 $\pm$ 0.09	0.07 $\pm$ 0.03	0.17 $\pm$ 0.03
	<b>Ridge</b>	0.07 $\pm$ 0.06	0.12 $\pm$ 0.01	0.05 $\pm$ 0.01		0.46 $\pm$ 0.06	0.06 $\pm$ 0.08	0.02 $\pm$ 0.01	0.07 $\pm$ 0.04	0.12 $\pm$ 0.02	0.1 $\pm$ 0.01	0.2 $\pm$ 0.01
	<b>wLasso</b>	0.0 $\pm$ 0.01	0.13 $\pm$ 0.04	0.08 $\pm$ 0.04		0.0 $\pm$ 0.01	-0.15 $\pm$ 0.12	0.0 $\pm$ 0.02	0.02 $\pm$ 0.04	0.14 $\pm$ 0.06	0.04 $\pm$ 0.04	0.18 $\pm$ 0.03
	<b>Lasso</b>	0.02 $\pm$ 0.03	0.12 $\pm$ 0.01	0.06 $\pm$ 0.01		0.38 $\pm$ 0.06	0.0 $\pm$ 0.01	0.02 $\pm$ 0.01	0.02 $\pm$ 0.02	0.12 $\pm$ 0.02	0.1 $\pm$ 0.01	0.2 $\pm$ 0.01
	<b>GLM</b>	0.09 $\pm$ 0.05	0.05 $\pm$ 0.01	0.04 $\pm$ 0.01		0.23 $\pm$ 0.04	-0.11 $\pm$ 0.07	0.01 $\pm$ 0.01	0.04 $\pm$ 0.04	0.04 $\pm$ 0.02	0.06 $\pm$ 0.01	0.07 $\pm$ 0.01

Site	Method	Aged salt	Biomass burning	Dust	HFO	Industrial	MSA rich	Nitrate rich	Primary biogenic	Salt	Sulfate rich	Road traffic
CHAM	<b>OLS</b>		0.09±0.01	0.11±0.02		0.2±0.06	0.12±0.04	0.14±0.02	0.11±0.02	0.05±0.03	0.36±0.06	
	<b>WLS</b>		0.09±0.01	0.09±0.01		0.24±0.04	0.07±0.02	0.13±0.01	0.11±0.02	0.08±0.01	0.39±0.04	
	<b>wPLS</b>		0.09±0.01	0.09±0.01		0.24±0.04	0.07±0.02	0.13±0.01	0.11±0.02	0.08±0.01	0.39±0.04	
	<b>PLS</b>		0.09±0.01	0.11±0.02		0.2±0.06	0.12±0.04	0.14±0.02	0.11±0.02	0.06±0.02	0.36±0.06	
	<b>wRidge</b>		0.09±0.01	0.09±0.01		0.24±0.04	0.07±0.02	0.13±0.01	0.11±0.02	0.08±0.01	0.39±0.04	
	<b>Ridge</b>		0.09±0.01	0.11±0.02		0.2±0.06	0.12±0.04	0.14±0.02	0.11±0.02	0.05±0.03	0.36±0.06	
	<b>wLasso</b>		0.09±0.01	0.09±0.01		0.12±0.04	0.06±0.02	0.12±0.01	0.1±0.02	0.08±0.01	0.38±0.04	
	<b>Lasso</b>		0.09±0.01	0.11±0.02		0.07±0.05	0.11±0.04	0.13±0.02	0.1±0.02	0.05±0.03	0.35±0.06	
	<b>GLM</b>		0.03±0.0	0.02±0.01		-0.05±0.04	0.05±0.01	0.06±0.01	0.05±0.01	-0.0±0.02	0.07±0.03	
RBX	<b>OLS</b>	0.03±0.03	0.1±0.03	0.25±0.01		-0.01±0.04	0.06±0.01	0.06±0.03	0.06±0.02	-0.09±0.03	0.14±0.02	
	<b>WLS</b>	-0.0±0.04	-0.03±0.03	0.25±0.01		-0.12±0.06	0.07±0.01	0.01±0.03	0.0±0.04	-0.11±0.04	0.19±0.02	
	<b>wPLS</b>	0.02±0.02	0.01±0.02	0.23±0.01		0.01±0.03	0.06±0.01	0.03±0.02	0.01±0.02	0.0±0.0	0.23±0.02	
	<b>PLS</b>	0.03±0.02	0.1±0.03	0.25±0.01		0.02±0.03	0.05±0.01	0.06±0.02	0.07±0.02	0.0±0.0	0.15±0.01	
	<b>wRidge</b>	-0.0±0.04	-0.03±0.03	0.25±0.01		-0.12±0.06	0.07±0.01	0.01±0.03	0.0±0.04	-0.11±0.04	0.19±0.02	
	<b>Ridge</b>	0.03±0.03	0.1±0.03	0.25±0.01		-0.01±0.04	0.06±0.01	0.06±0.03	0.06±0.02	-0.09±0.03	0.14±0.02	
	<b>wLasso</b>	-0.0±0.04	-0.02±0.03	0.25±0.01		-0.09±0.05	0.06±0.01	0.01±0.02	0.0±0.03	-0.1±0.04	0.19±0.02	
	<b>Lasso</b>	0.02±0.02	0.1±0.03	0.25±0.01		-0.01±0.03	0.06±0.01	0.05±0.02	0.06±0.02	-0.09±0.03	0.14±0.02	
	<b>GLM</b>	0.01±0.02	0.02±0.01	0.06±0.01		0.02±0.01	0.02±0.0	0.04±0.01	0.02±0.01	-0.02±0.01	0.05±0.0	
NIC	<b>OLS</b>	0.09±0.02	0.12±0.01	0.1±0.02		0.07±0.02	0.16±0.02	0.01±0.03	0.07±0.02	0.07±0.01	0.34±0.05	
	<b>WLS</b>	0.11±0.02	0.12±0.01	0.11±0.02		0.05±0.02	0.09±0.03	0.01±0.04	0.12±0.04	0.08±0.02	0.28±0.06	
	<b>wPLS</b>	0.11±0.02	0.12±0.01	0.11±0.02		0.05±0.02	0.09±0.03	0.02±0.02	0.12±0.04	0.08±0.02	0.28±0.06	
	<b>PLS</b>	0.09±0.02	0.12±0.01	0.09±0.01		0.07±0.02	0.16±0.02	0.01±0.02	0.07±0.02	0.07±0.01	0.34±0.05	
	<b>wRidge</b>	0.11±0.02	0.12±0.01	0.11±0.02		0.05±0.02	0.09±0.03	0.01±0.04	0.12±0.04	0.08±0.02	0.28±0.06	
	<b>Ridge</b>	0.09±0.02	0.12±0.01	0.1±0.02		0.07±0.02	0.16±0.02	0.01±0.03	0.07±0.02	0.07±0.01	0.34±0.05	
	<b>wLasso</b>	0.12±0.02	0.12±0.01	0.11±0.02		0.04±0.02	0.08±0.03	0.0±0.02	0.11±0.04	0.08±0.02	0.25±0.06	
	<b>Lasso</b>	0.08±0.02	0.12±0.01	0.1±0.01		0.06±0.02	0.15±0.02	0.0±0.01	0.05±0.02	0.07±0.01	0.31±0.05	
	<b>GLM</b>	0.05±0.01	0.04±0.0	0.04±0.01		0.03±0.01	0.05±0.01	-0.0±0.02	0.03±0.01	0.03±0.01	0.17±0.03	

## Intrinsic OP of the best and the reference model

Table S. 8. Intrinsic PM<sub>10</sub>OP<sub>DTT</sub> (nmol min<sup>-1</sup> µg<sup>-1</sup>) of the best and the reference model

<b>Method</b>	<b>Sources</b>	<b>count</b>	<b>mean</b>	<b>std</b>	<b>min</b>	<b>25%</b>	<b>50%</b>	<b>75%</b>	<b>max</b>	<b>IQR</b>
<b>Best</b>	Aged salt	2500	0.043	0.043	-0.023	0	0.030	0.076	0.264	0.076
<b>OLS</b>	Aged salt	2500	0.041	0.046	-0.095	0.007	0.032	0.076	0.264	0.069
<b>Best</b>	Biomass burning	3000	0.122	0.029	0.009	0.100	0.120	0.137	0.207	0.037
<b>OLS</b>	Biomass burning	3000	0.123	0.030	-0.003	0.099	0.120	0.140	0.207	0.041
<b>Best</b>	Dust	3000	0.124	0.069	0.007	0.076	0.097	0.168	0.291	0.092
<b>OLS</b>	Dust	3000	0.122	0.070	-0.015	0.060	0.104	0.169	0.291	0.109
<b>Best</b>	HFO	500	0.183	0.015	0.142	0.173	0.183	0.192	0.233	0.019
<b>OLS</b>	HFO	500	0.183	0.015	0.142	0.173	0.183	0.192	0.233	0.019
<b>Best</b>	Industrial	1000	0.045	0.033	-0.020	0.023	0.039	0.059	0.181	0.036
<b>OLS</b>	Industrial	1000	0.030	0.028	-0.068	0.012	0.030	0.047	0.139	0.035
<b>Best</b>	MSA rich	3000	0.109	0.088	0	0.040	0.079	0.186	0.502	0.146
<b>OLS</b>	MSA rich	3000	0.099	0.087	-0.140	0.040	0.085	0.170	0.502	0.129
<b>Best</b>	Nitrate rich	3000	0.053	0.052	0	0.019	0.036	0.070	0.211	0.051
<b>OLS</b>	Nitrate rich	3000	0.066	0.056	-0.055	0.021	0.040	0.122	0.211	0.101
<b>Best</b>	Primary biogenic	2500	0.101	0.062	-0.069	0.053	0.123	0.142	0.268	0.089
<b>OLS</b>	Primary biogenic	2500	0.116	0.081	-0.110	0.053	0.127	0.159	0.418	0.107
<b>Best</b>	Road traffic	2500	0.279	0.098	0.107	0.191	0.296	0.361	0.588	0.169
<b>OLS</b>	Road traffic	2500	0.272	0.097	0.066	0.192	0.291	0.344	0.560	0.153
<b>Best</b>	Salt	3000	0.086	0.030	0	0.064	0.084	0.109	0.183	0.045
<b>OLS</b>	Salt	3000	0.080	0.035	0	0.051	0.081	0.105	0.204	0.054
<b>Best</b>	Sulfate rich	3000	0.071	0.039	0	0.058	0.077	0.094	0.233	0.037
<b>OLS</b>	Sulfate rich	3000	0.066	0.086	-0.219	0.050	0.075	0.100	0.358	0.049

Table S. 9. Intrinsic PM<sub>10</sub>OP<sub>AA</sub> (nmol min<sup>-1</sup> µg<sup>-1</sup>) of the best and the reference model

<b>Method</b>	<b>Sources</b>	<b>count</b>	<b>mean</b>	<b>Std</b>	<b>min</b>	<b>25%</b>	<b>50%</b>	<b>75%</b>	<b>max</b>	<b>IQR</b>
<b>Best</b>	Road traffic	2500	0.245	0.064	0.093	0.199	0.231	0.275	0.492	0.076
<b>OLS</b>	Road traffic	2500	0.226	0.079	-0.063	0.171	0.210	0.265	0.526	0.094
<b>OLS</b>	Biomass burning	3000	0.198	0.092	0.079	0.120	0.164	0.281	0.400	0.161
<b>Best</b>	Biomass burning	3000	0.192	0.083	0.078	0.123	0.163	0.278	0.410	0.156
<b>Best</b>	HFO	500	0.120	0.011	0.089	0.113	0.121	0.127	0.153	0.014
<b>OLS</b>	HFO	500	0.120	0.012	0.087	0.112	0.121	0.128	0.154	0.015
<b>OLS</b>	Aged salt	2500	0.083	0.115	-0.032	0.023	0.042	0.063	0.509	0.041
<b>Best</b>	Aged salt	2500	0.055	0.063	-0.039	0.016	0.038	0.058	0.299	0.042
<b>Best</b>	Salt	3000	0.043	0.036	-0.007	0.015	0.029	0.067	0.159	0.052
<b>OLS</b>	Salt	3000	0.042	0.071	-0.156	0.011	0.026	0.096	0.238	0.085
<b>Best</b>	Primary biogenic	3000	0.020	0.032	-0.114	0	0.026	0.042	0.110	0.042
<b>OLS</b>	Primary biogenic	3000	0.021	0.042	-0.150	-0.007	0.021	0.039	0.145	0.046
<b>Best</b>	Industrial	1000	0.020	0.013	0	0.011	0.019	0.028	0.074	0.016
<b>OLS</b>	Industrial	1000	0.017	0.017	-0.045	0.006	0.016	0.027	0.087	0.021
<b>OLS</b>	Dust	3000	0.026	0.045	-0.069	-0.001	0.012	0.027	0.160	0.027
<b>Best</b>	Dust	3000	0.027	0.043	-0.041	0	0.011	0.025	0.160	0.025

<b>OLS</b>	MSA_rich	3000	0.029	0.067	-0.248	-0.018	0.006	0.076	0.324	0.093
<b>Best</b>	Sulfate_rich	3000	0.005	0.015	-0.063	0	0.005	0.014	0.055	0.014
<b>Best</b>	MSA_rich	3000	0.035	0.055	-0.047	0	0.002	0.064	0.307	0.064
<b>OLS</b>	Sulfate_rich	3000	-0.008	0.027	-0.122	-0.026	0.002	0.012	0.051	0.037
<b>Best</b>	Nitrate_rich	3000	0.002	0.012	-0.064	0	0	0.006	0.035	0.006
<b>OLS</b>	Nitrate_rich	3000	-0.005	0.020	-0.309	-0.013	-0.006	0.007	0.035	0.020

## Similarity between the chemical profile of sources

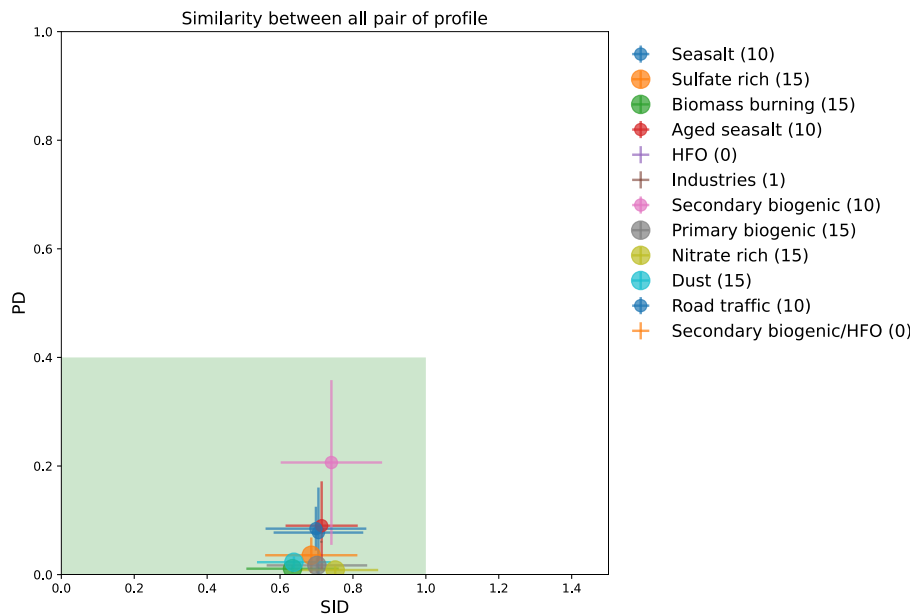


Figure S. 13. Similarity between the chemical profile of sources

## Contribution of sources to PM in 6 sites

Table S. 10. Contribution of sources ( $\mu\text{g m}^{-3}$ ) to PM in 6 sites

	PdB	TAL	GRE-fr	CHAM	RBX	NIC
<b>Aged seasalt</b>	10.14	8.91	2.96		9.64	9.32
<b>Biomass burning</b>	13.07	18.60	15.70	45.56	9.90	15.32
<b>Dust</b>	12.35	13.94	13.85	8.56	18.85	20.92
<b>HFO</b>	8.73					
<b>Industries</b>	5.38	11.10	1.72			
<b>Nitrate rich</b>	11.34	18.72	14.52	7.77	27.92	7.98
<b>Primary biogenic</b>	11.27	4.27	3.89	11.57	4.92	6.22
<b>Road traffic</b>		7.02	14.12	5.40	10.43	8.69
<b>Seasalt</b>	6.57	8.02	4.28	7.12	6.19	5.60
<b>Secondary biogenic</b>	5.82	3.54	1.25	1.68	3.88	10.21
<b>Sulfate rich</b>	15.32	5.88	27.69	12.34	8.26	15.73

## S1. Hyperparameter of RF and MLP

### S1.1. Random forest

Hyperparameter tuning was implemented by using a 5-fold cross-validation to identify the best hyperparameter for OP prediction in every site. A grid search cross-validation technique was applied on a list of hyperparameters, which are: number of the decision tree in forest, the minimum number of samples required to split on an internal node and to be a leaf node, the maximum possible depth of each tree and create a multiple randomly decision tree or not (table S.11). The hyperparameter of the best performance are different across sites, especially in the number of trees. However, the change in the hyperparameter did not change much the model accuracy, therefore, a set of similar hyperparameters was chosen for 6 sites to simply and reduce the time of running the model.

Table S. 11. Hyperparameter tuning

	Hyperparameter tuning	Best hyperparameter (for all sites)
n_estimators	20, 50, 100	20
min_samples_split	2, 4, 6, 8, 10	2
min_samples_leaf	1, 2, 3, 4	1
max_depth	11, 12, 13, 14, 15, ..20	14
bootstrap	True, False	True

### S1.2. Multiple-layer perceptron

Applying the same processes as RF, a set hyperparameter of MLP was chosen for tuning, including: the activation function represent to the relationships within the data, the solver for weight optimization, and maximum number of iterations (Table S.12). The best hyperparameter for OP prediction are the same for all the sites. A 2-hidden layer, the first containing 64 neurons and the second 32 was chosen without running the hyperparameter to diminish the time computation.

Table S. 12. Hyperparameter tuning

	Hyperparameter tuning	Best hyperparameter (for all sites)
max_iter	20, 50, 100	50
activation	tanh, relu, logistic	logistic
solver	sg, adam, lbfgs	lbfgs
hidden_layer_sizes	X	(64, 32)

## S2. Comparison of intrinsic PM<sub>10</sub> OP<sub>AA</sub> between the best and reference models

### Group 1: Anthropogenic sources

The first category consisted of anthropogenic sources, with the highest intrinsic OP values in the best and reference models. Among these sources, road traffic (best model:  $0.24 \pm 0.06$ ; OLS:  $0.23 \pm 0.08$ ) emerged as the most prominent contributor, followed by biomass burning (best model:  $0.19 \pm 0.08$ , OLS:  $0.2 \pm 0.08$ ), HFO (best model:  $0.12 \pm 0.01$ , HFO:  $0.12 \pm 0.01$ ), and industrial (best model:  $0.02 \pm 0.01$ , OLS:  $0.02 \pm 0.02$ ). These results are following prior research (Calas et al., 2019; Dominutti et al., 2023; Fadel et al., 2023; Fang et al., 2016; in 't Veld et al., 2023a; Weber et al., 2018; Zhang et al., 2020) which has highlighted the sensitivity of OP<sub>AA</sub> to concentrations of metals, black carbon and organic carbon. The differences between the best and reference models were insignificant for these sources, demonstrating that the best and reference models consistently captured similar patterns for the most critical sources of OP activities. However, the best model displayed slightly reduced variability across sites.

## Group 2: Natural inorganic sources

The second group included aged sea salt, sea salt, and dust sources, each characterized by their intrinsic OP values (in  $\text{nmol} \cdot \text{min}^{-1} \cdot \mu\text{g}^{-1}$ ). The intrinsic OP values for aged sea salt were  $0.05 \pm 0.06$  in the best model and  $0.08 \pm 0.11$  in the OLS model. In the best and OLS models, sea salt exhibited intrinsic OP values of  $0.05 \pm 0.04$  and  $0.04 \pm 0.07$ , respectively. The source of dust had Intrinsic OP values of  $0.03 \pm 0.04$  in the best model and  $0.03 \pm 0.05$  in the OLS model. The median intrinsic OP values between the best and reference models remained relatively consistent. However, significant differences were observed in the mean Intrinsic OP values across individual sites. These disparities were primarily attributed to substantial variations in the Intrinsic OP values of individual sites between the best and OLS models, with the most pronounced differences observed in fresh and aged sea salt sources.

While most sites exhibited shallow intrinsic OP values for aged sea salt, GRE-fr, in the OLS model, returned a notably high intrinsic OP value of 0.30, surpassing even road traffic (0.16). The best model, however, mitigated the impact of aged sea salt, resulting in a more reasonable intrinsic OP value of 0.17, which was less significant than biomass burning (0.3) and traffic (0.19). As suggested in previous research, this elevated intrinsic OP value for aged sea salt in GRE-fr can be attributed to potentially toxic components mixed with salts actually used for road salting in winter, especially during severe thermal inversion events in the valley environments (Favez et al., 2010; Borlaza et al., 2021; Scotto et al., 2021; Caserini et al., 2017). These studies have indicated that during thermal inversion events, a layer of warm air traps cooler air near the ground, accumulating pollutants over time, potentially during thermal inversion events through photochemical reactions.

High proportions of  $\text{Na}^+$  and  $\text{Cl}^-$  were detected in sea salt, components typically associated with limited effects on oxidative potential (OP) activities. However, a notable anomaly was identified in GRE-fr, where the OLS model yielded a negative intrinsic OP for salt (-0.07). In contrast, the other sites exhibited a range of intrinsic OP values for sea salt, varying from 0.01 to 0.15. When employing the best model, the intrinsic OP for salt in GRE-fr was increased to 0.01, aligning it more closely with the values observed at other sites. Intrinsic OP in the best model brought a more consistent range of sea salt intrinsic OP across all sites.

The intrinsic OP of the dust source across the combined six sites and individual sites displayed minimal variability between the two models. Remarkably, the RBX model consistently yielded a substantial intrinsic OP value for dust (0.12 in both models), likely due to the mixture of crustal dust with an industrial source containing a high proportion of metals (see SI for details). Within this group, the best model outperformed the OLS method by exhibiting less variation across sites.

## Biogenic sources

The third group comprised two biogenic sources: primary biogenic and marine secondary biogenic oxidation (MSA rich). These sources were highlighted in very few studies as well as their OP contribution. Both primary biogenic and MSA-rich sources were detected in all six sites, thanks to their trace species, Polyols and MSA. However, in this study, primary biogenic in RBX was excluded to ensure consistency because the measurement method differed in RBX. These two sources represent complex biogenic atmospheric processes subject to limited research on their redox properties. However, combining the best model facilitated attaining more comparable Intrinsic OP values for these sources across sites.

The median intrinsic OP values for the best and OLS models of primary biogenic sources exhibited non-negative intrinsic values (best method:  $0.03 \pm 0.02$ , reference method:  $0.02 \pm 0.05$ ). However, the mean intrinsic OP values for individual sites revealed a negative intrinsic OP in NIC (-0.03). This negative value represented a 100% reduction compared to all sites, mean Intrinsic OP encompassing. It is noteworthy that prior research by Samake (2017) demonstrated that bacteria could reduce OP activities

by a maximum of 60%, and fungi could increase OP activities by up to 30%. This suggests that the negative intrinsic OP observed in NIC was likely due to the unrespecting of the OLS assumptions, affecting the model results.

The intrinsic OP of MSA-rich sources displayed notable variability across sites in both the best and reference models (best model:  $0.099 \pm 0.087$ , reference model:  $0.109 \pm 0.088$ ). Originating as a product of marine phytoplankton emissions, this source exhibited mixing with specific marine constituents, including  $\text{Na}^+$ ,  $\text{Cl}^-$ , V, and Ni. Furthermore, MSA particles are more dominant in PM<sub>2.5</sub> fraction, facilitating long-range transport and incorporation with other secondary or aged particles. The long-range transport process and aging components within these particles may introduce redox-active elements, potentially accounting for the elevated intrinsic OP of this source observed in valley sites GRE-fr and CHAM across both the best and reference models.

#### Secondary inorganic aerosol

The final group included secondary nitrate and sulfate sources, which exhibited crucial disparities between the best and reference methods. The Intrinsic OP of nitrate demonstrated the lowest values (best model:  $0.005 \pm 0.01$ , reference model:  $-0.005 \pm 0.02$ ), followed by sulfate (best model:  $0.005 \pm 0.01$ , reference model:  $-0.008 \pm 0.03$ ). Secondary inorganic sources are recognized for their minimal influence on OP activity, leading to a low intrinsic OP, as discussed in previous studies (Fadel et al., 2023; Dominutti et al., 2023; Daellenbach et al., 2020; Weber et al., 2021).

The sulfate-rich component exhibited distinct characteristics in the best model compared to the reference model. The best model had a remarkable alignment between the mean and median values. Conversely, the reference model displayed a negative mean and a positive median for sulfate-rich Intrinsic OP. Within the OLS model, individual sites yielded significantly negative values for the mean (CHAM: -0.05, TAL: -0.02, RBX: -0.02), while in the best model, most sites exhibited positive Intrinsic OP (CHAM: 0.009; GRE-fr: 0.019; NIC: 0.006; PdB: 0.003; TAL: 0.00), except for RBX (-0.018). The negative intrinsic value observed in sulfate-rich at RBX may be attributed to the notably low proportion of organic carbon (OC) content, accounting for only 5% in RBX compared to higher percentages in other sites (33% in GRE-fr, 10% in CHAM and PdB, 9% in NIC). TAL, did not exhibit the lowest Intrinsic OP despite having a low OC proportion (2%) in its chemical profile, possibly due to the presence of nickel (Ni) and vanadium (V), which may be associated with shipping activities.

In the best model, the intrinsic OP of nitrate-rich sources also demonstrated greater consistency across sites compared to the reference models. The best model returned similar intrinsic OP values around 0 for all sites except RBX. In contrast, the OLS model exhibited variations in intrinsic OP values (CHAM: -0.014; GRE-fr: -0.010; NIC: -0.013; PdB: -0.009; RBX: 0.02; TAL: 0.005). Although nitrate is generally considered to have no significant impact on OP activities (Daellenbach et al., 2020), one would expect all sites to exhibit similar intrinsic OP values. However, the higher intrinsic OP values in RBX can be attributed to an industrial source in this site (containing As, Cd, Cs), which can react with  $\text{OP}_{\text{AA}}$ , leading to the observed differences.

### S3. Correlation between $\text{PM}_{10}$ $\text{OP}_v$ , $\text{PM}_{10}$ $\text{OP}_m$ and PM mass concentration

Table S. 13. The coefficient determination of  $\text{PM}_{10}$   $\text{OP}_v$  vs PM mass concentration and of  $\text{PM}_{10}$   $\text{OP}_m$  and PM mass concentration

	<b>GRE-fr</b>	<b>CHAM</b>	<b>NIC</b>	<b>PdB</b>	<b>RBX</b>	<b>TAL</b>
<b><math>\text{OP}_{\text{AA}}^{\text{v}}</math></b>	0.68	0.55	0.35	0.36	0.62	0.69
<b><math>\text{OP}_{\text{AA}}^{\text{m}}</math></b>	0.10	-0.04	-0.15	-0.03	-0.27	0.07

$\text{OP}_{\text{DTT}}^{\text{v}}$	0.78	0.86	0.75	0.58	0.83	0.68
$\text{OP}_{\text{DTT}}^{\text{m}}$	0.09	0.00	-0.34	-0.08	-0.12	-0.20

### Contribution of sources to $\text{PM}_{10} \text{OP}_{\text{AA}}^{\text{v}}$ , $\text{PM}_{10} \text{OP}_{\text{DTT}}^{\text{v}}$ and $\text{PM}_{10}$

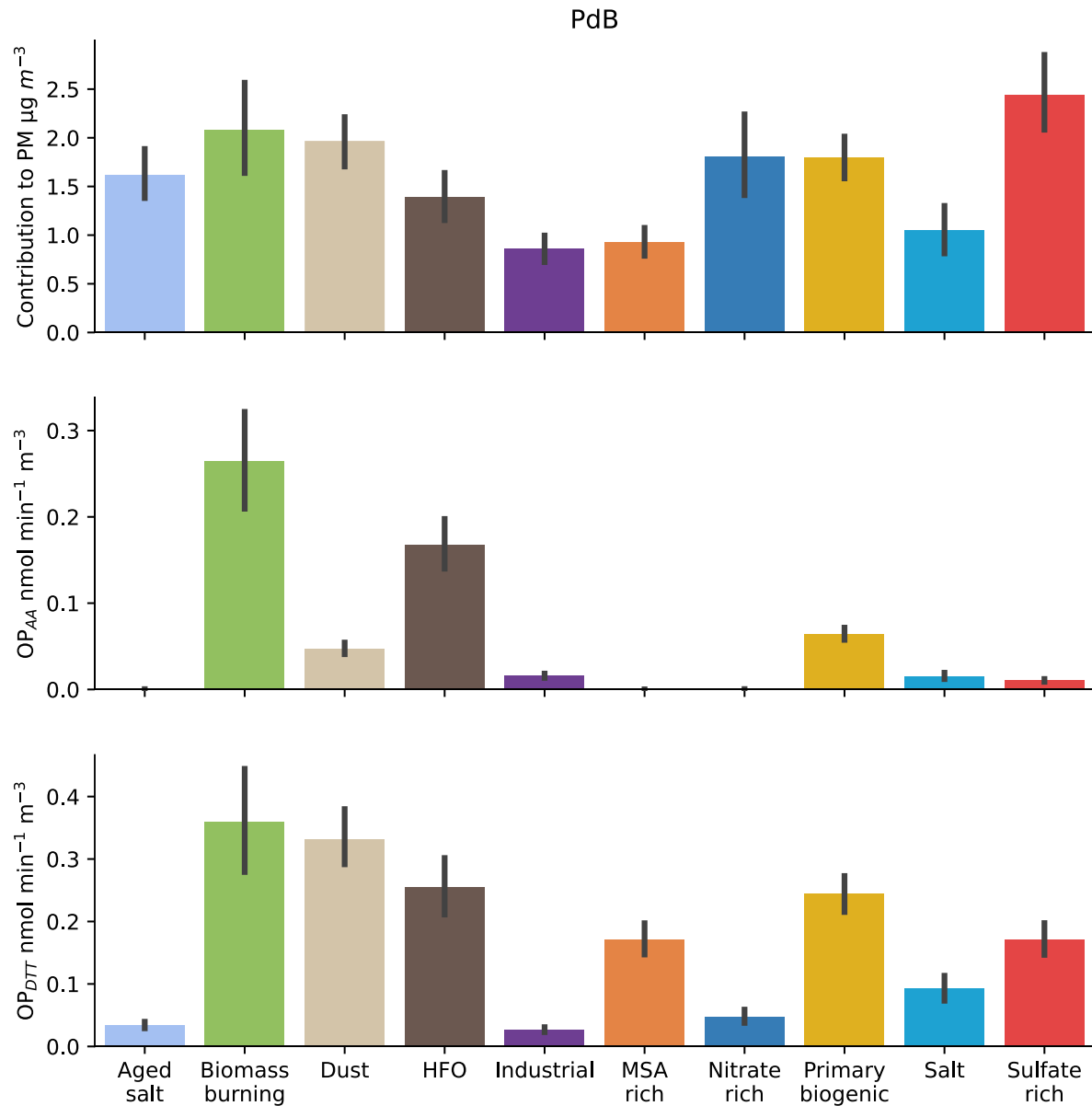


Figure S. 14. Daily mean contribution of sources to  $\text{PM}_{10}$ ,  $\text{PM}_{10} \text{OP}_{\text{AA}}$  and  $\text{PM}_{10} \text{OP}_{\text{DTT}}$  in PdB. The error bar denotes the 95% interval of the mean values.

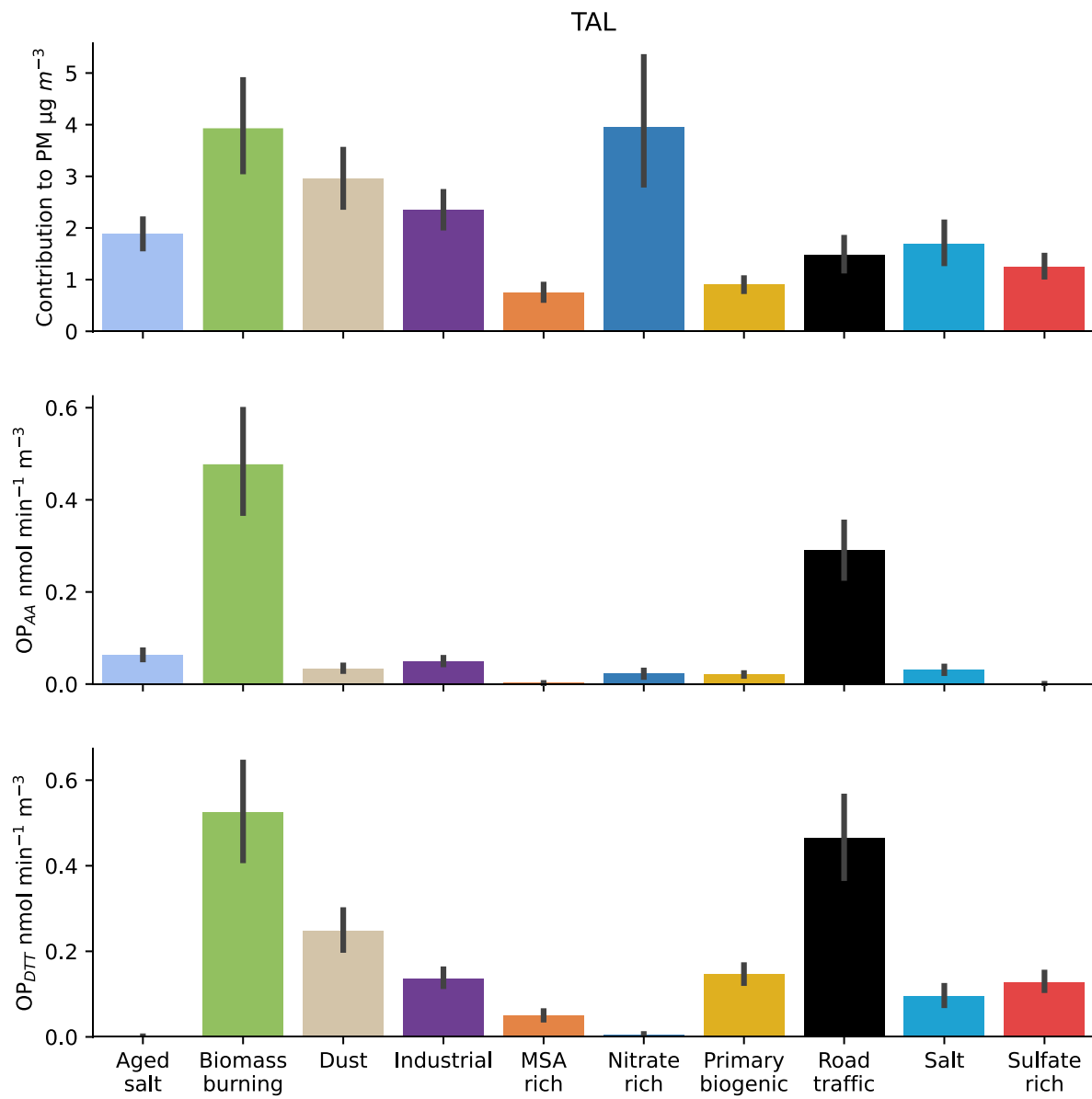


Figure S. 15. Daily mean contribution of sources to  $\text{PM}_{10}$ ,  $\text{PM}_{10}\text{OP}_{\text{AA}}$  and  $\text{PM}_{10}\text{OP}_{\text{DTT}}$  in TAL. The error bar denotes the 95% interval of the mean values.

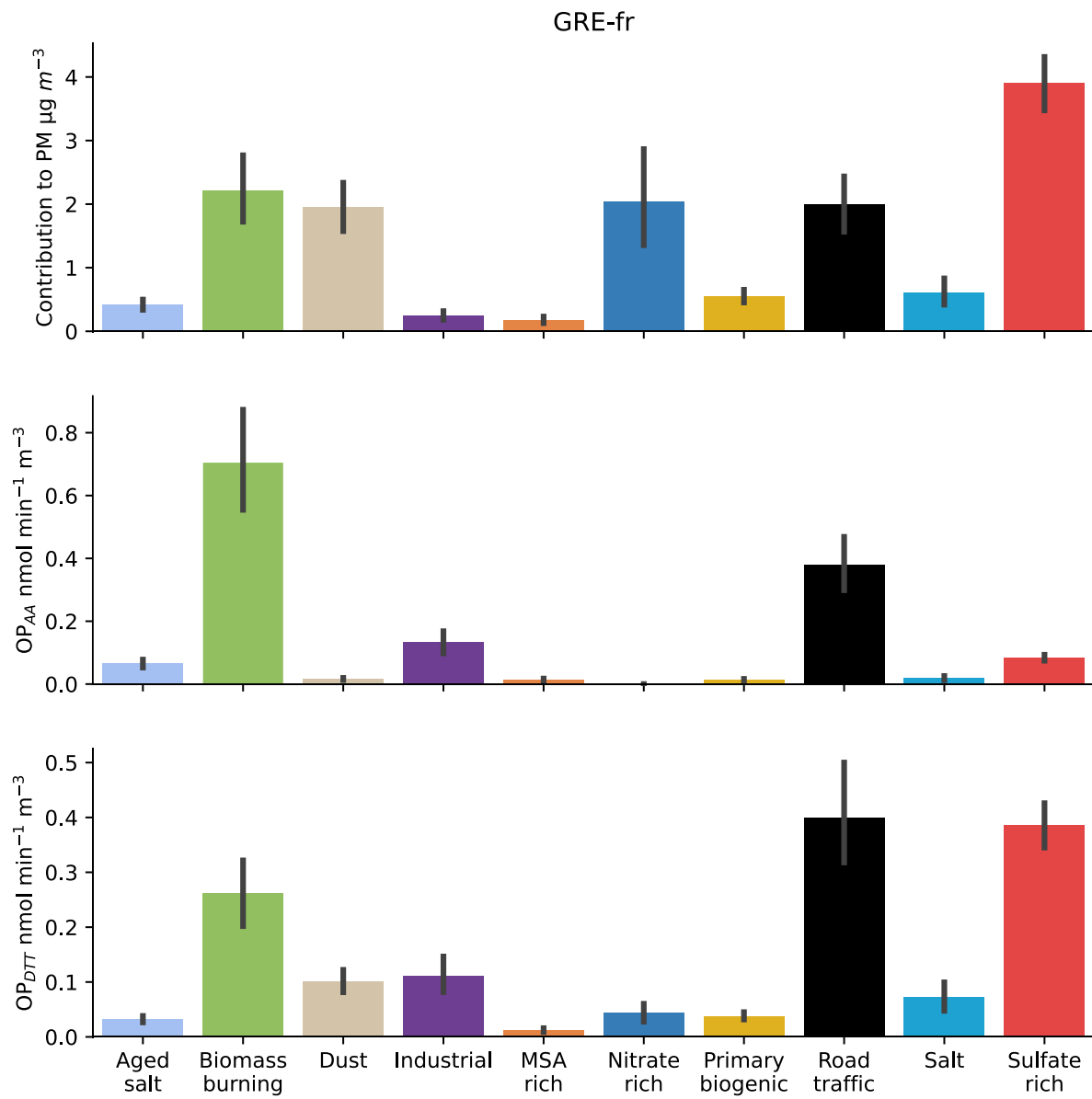


Figure S. 16. Daily mean contribution of sources to  $\text{PM}_{10}$ ,  $\text{PM}_{10} \text{OP}_{\text{AA}}$  and  $\text{PM}_{10} \text{OP}_{\text{DTT}}$  in GRE-fr. The error bar denotes the 95% interval of the mean values.

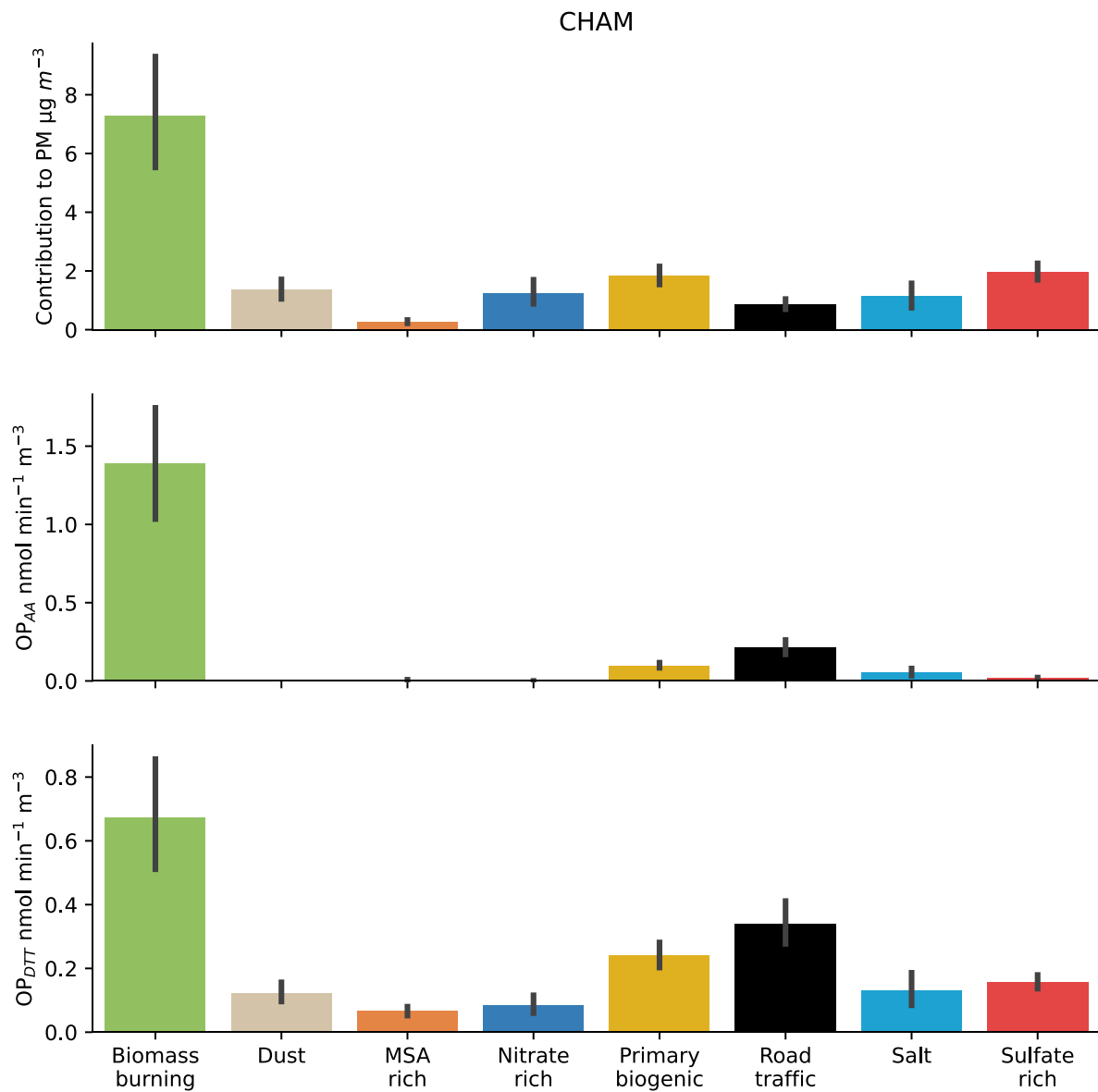


Figure S. 17. Daily mean contribution of sources to  $\text{PM}_{10}$ ,  $\text{PM}_{10} \text{OP}_{\text{AA}}$  and  $\text{PM}_{10} \text{OP}_{\text{DTT}}$  in CHAM. The error bar denotes the 95% interval of the mean values.

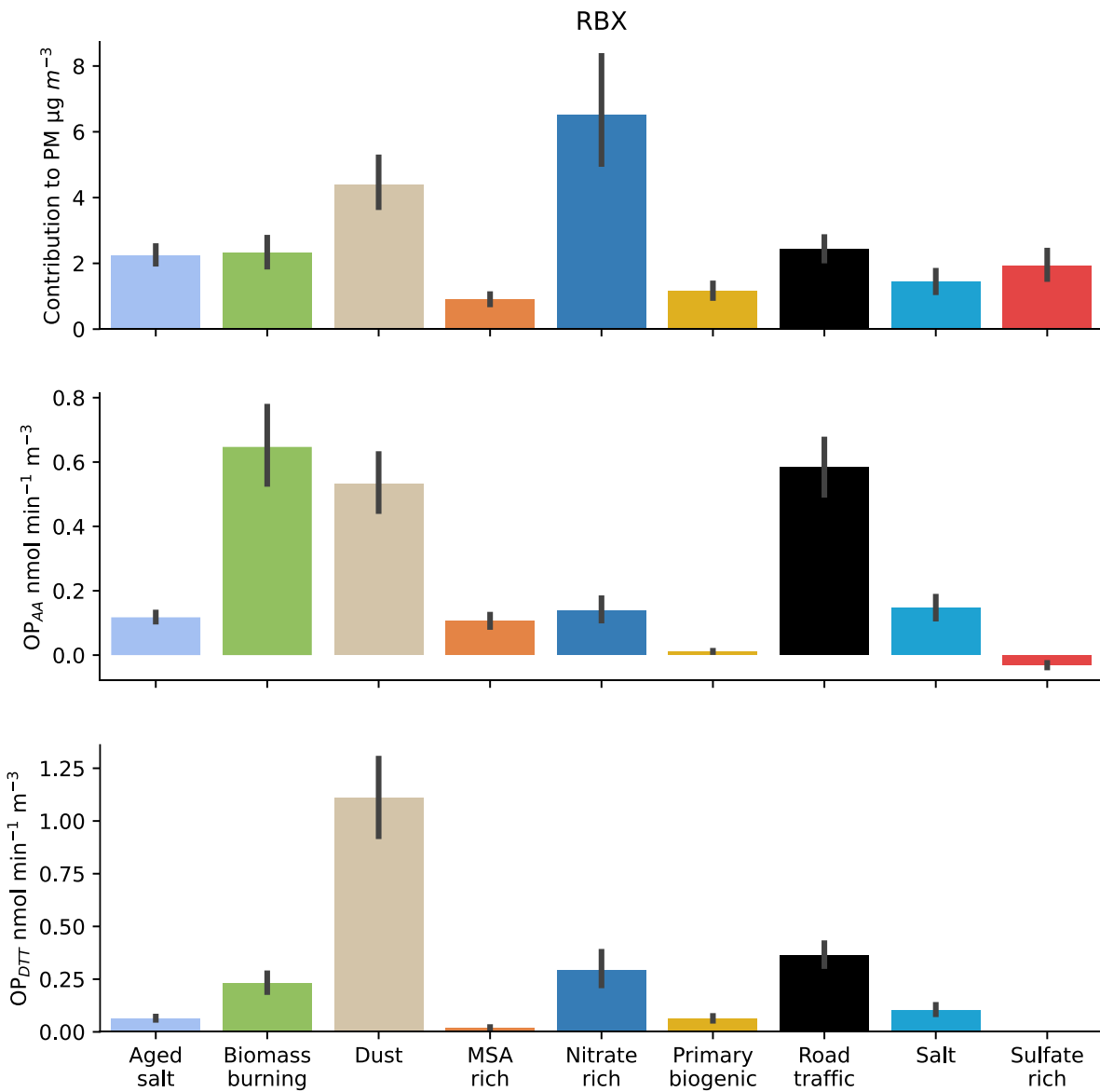


Figure S. 18. Daily mean contribution of sources to  $\text{PM}_{10}$ ,  $\text{PM}_{10} \text{OP}_{\text{AA}}$  and  $\text{PM}_{10} \text{OP}_{\text{DTT}}$  in RBX. The error bar denotes the 95% interval of the mean values.

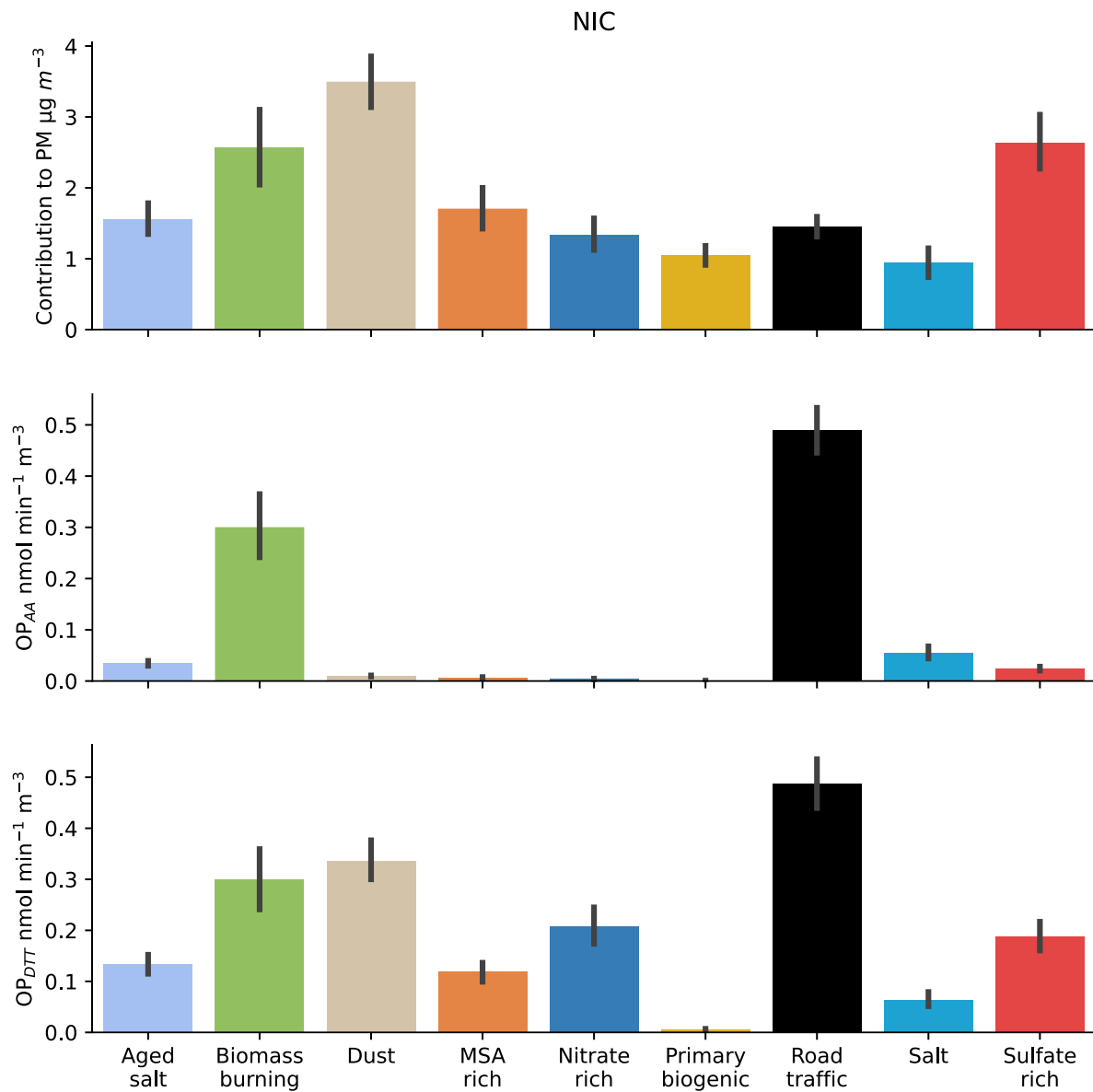


Figure S. 19. Daily mean contribution of sources to  $\text{PM}_{10}$ ,  $\text{PM}_{10} \text{OP}_{\text{AA}}$  and  $\text{PM}_{10} \text{OP}_{\text{DTT}}$  in NIC. The error bar denotes the 95% interval of the mean values.

## Chemical profile of Sea salt, sulfate-rich and nitrate-rich in NIC

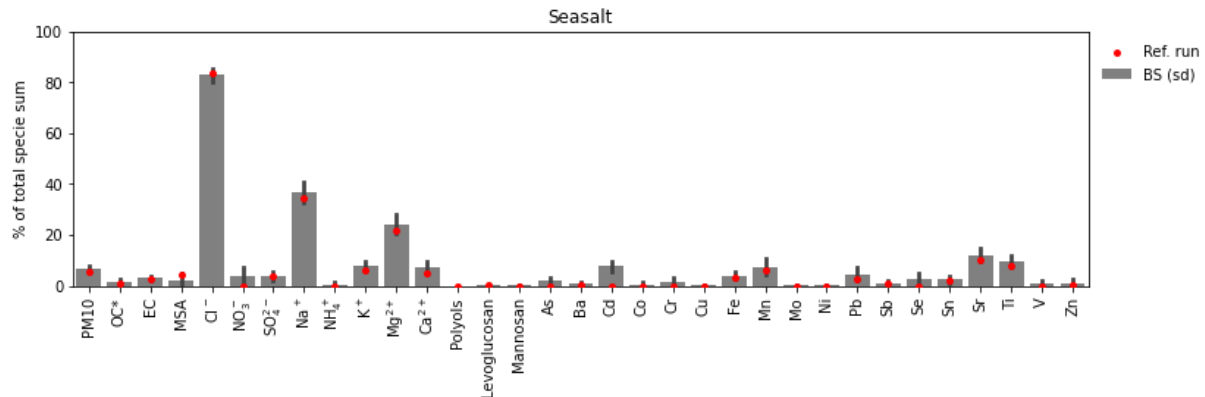


Figure S. 20. Chemical of seasalt in NIC. The red dot indicates the percentage of total species in the reference run, the bar denotes the mean and standard deviation values of 100 bootstrap runs. The figure was performed using the PyPMF package version 0.1.12 (Weber et al., 2018).

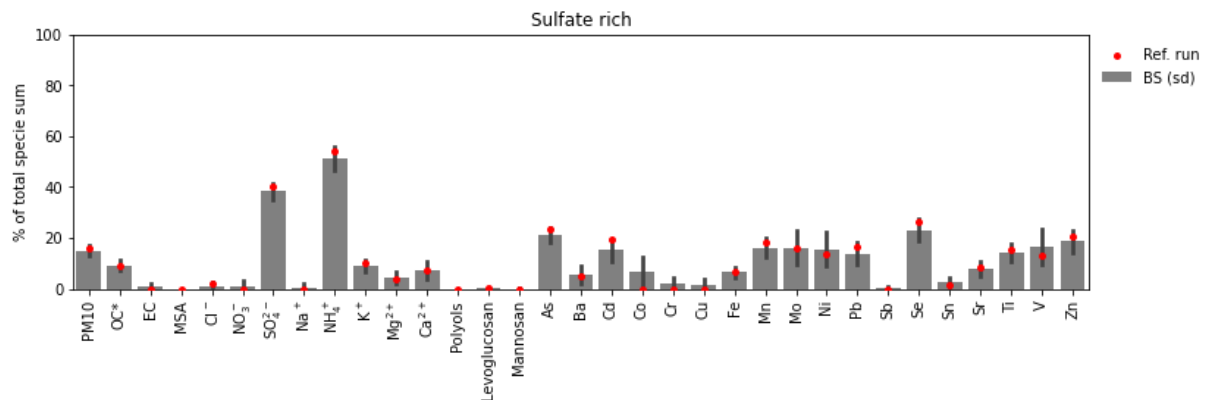


Figure S. 21. Chemical of sulfate rich in NIC. The red dot indicates the percentage of total species in the reference run, the bar denotes the mean and standard deviation values of 100 bootstrap runs. The figure was performed using the PyPMF package version 0.1.12 (Weber et al., 2018).

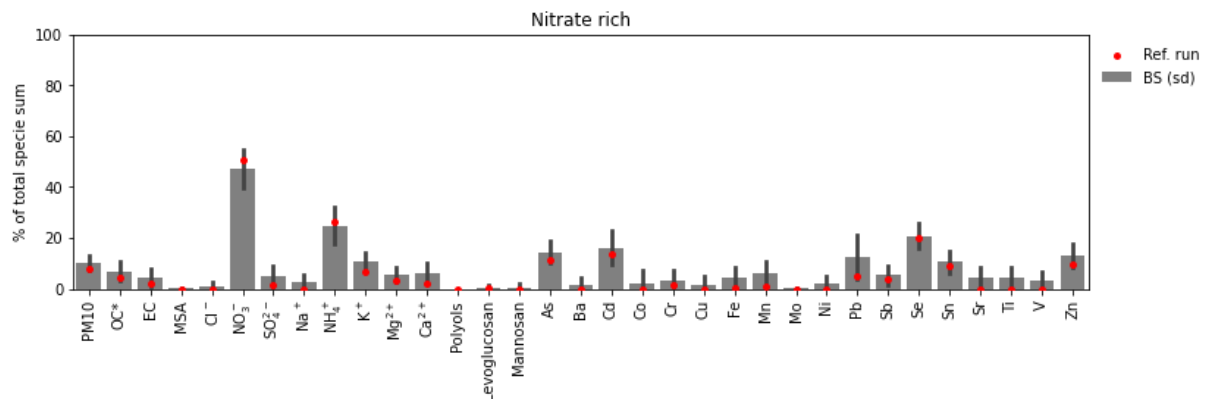


Figure S. 22. Chemical of nitrate rich in NIC. The red dot indicates the percentage of total species in the reference run, the bar denotes the mean and standard deviation values of 100 bootstrap runs. The figure was performed using the PyPMF package version 0.1.12 (Weber et al., 2018).

## Reference

- Borlaza, L., Weber, S., Uzu, G., Jacob, V., Cañete, T., Micallef, S., Trébuchon, C., Slama, R., Favez, O., and Jaffrezo, J.-L.: Disparities in particulate matter (PM10) origins and oxidative potential at a city scale (Grenoble, France) - Part 1: Source apportionment at three neighbouring sites, *Atmos. Chem. Phys.*, 21, 5415–5437, <https://doi.org/10.5194/acp-21-5415-2021>, 2021.
- Calas, A., Uzu, G., Besombes, J. L., Martins, J. M. F., Redaelli, M., Weber, S., Charron, A., Albinet, A., Chevrier, F., Brulfert, G., Mesbah, B., Favez, O., and Jaffrezo, J. L.: Seasonal variations and chemical predictors of oxidative potential (OP) of particulate matter (PM), for seven urban French sites, *Atmosphere (Basel)*, 10, <https://doi.org/10.3390/atmos10110698>, 2019.
- Caserini, S., Giani, P., Cacciamani, C., Ozgen, S., and Lonati, G.: Influence of climate change on the frequency of daytime temperature inversions and stagnation events in the Po Valley: historical trend and future projections, *Atmos. Res.*, 184, 15–23, <https://doi.org/10.1016/j.atmosres.2016.09.018>, 2017.
- Daellenbach, K. R., Uzu, G., Jiang, J., Cassagnes, L.-E., Leni, Z., Vlachou, A., Stefenelli, G., Canonaco, F., Weber, S., Segers, A., and Sources, al: Sources of particulate-matter air pollution and its oxidative potential in Europe of particulate-matter air pollution and its oxidative potential in Europe, *Nature*, 587, <https://doi.org/10.1038/s41586-020-2902-8>, 2020.
- Dominutti, P. A., Borlaza, L., Sauvain, J. J., Ngoc Thuy, V. D., Houdier, S., Suarez, G., Jaffrezo, J. L., Tobin, S., Trébuchon, C., Socquet, S., Moussu, E., Mary, G., and Uzu, G.: Source apportionment of oxidative potential depends on the choice of the assay: insights into 5 protocols comparison and implications for mitigation measures, *Environ. Sci. Atmos.*, <https://doi.org/10.1039/d3ea00007a>, 2023.
- Fadel, M., Courcot, D., Delmaire, G., Roussel, G., Afif, C., and Ledoux, F.: Source apportionment of PM<sub>2.5</sub> oxidative potential in an East Mediterranean site, *Sci. Total Environ.*, 900, <https://doi.org/10.1016/j.scitotenv.2023.165843>, 2023.
- Fang, T., Verma, V., T Bates, J., Abrams, J., Klein, M., Strickland, J. M., Sarnat, E. S., Chang, H. H., Mulholland, A. J., Tolbert, E. P., Russell, G. A., and Weber, J. R.: Oxidative potential of ambient water-soluble PM<sub>2.5</sub> in the southeastern United States: Contrasts in sources and health associations between ascorbic acid (AA) and dithiothreitol (DTT) assays, *Atmos. Chem. Phys.*, 16, 3865–3879, <https://doi.org/10.5194/acp-16-3865-2016>, 2016.
- Favez, O., El Haddad, I., Piot, C., Boréave, A., Abidi, E., Marchand, N., Jaffrezo, J. L., Besombes, J. L., Personnaz, M. B., Sciare, J., Wortham, H., George, C., and D'Anna, B.: Inter-comparison of source apportionment models for the estimation of wood burning aerosols during wintertime in an Alpine city (Grenoble, France), *Atmos. Chem. Phys.*, 10, 5295–5314, <https://doi.org/10.5194/acp-10-5295-2010>, 2010.
- Samake, A., Uzu, G., Martins, J. M. F., Calas, A., Vince, E., Parat, S., and Jaffrezo, J. L.: The unexpected role of bioaerosols in the Oxidative Potential of PM, *Sci. Rep.*, 7, <https://doi.org/10.1038/s41598-017-11178-0>, 2017.
- Scotto, F., Bacco, D., Lasagni, S., Trentini, A., Poluzzi, V., and Vecchi, R.: A multi-year source apportionment of PM<sub>2.5</sub> at multiple sites in the southern Po Valley (Italy), *Atmos. Pollut. Res.*, 12, <https://doi.org/10.1016/j.apr.2021.101192>, 2021.
- in 't Veld, M., Pandolfi, M., Amato, F., Pérez, N., Reche, C., Dominutti, P., Jaffrezo, J., Alastuey, A., Querol, X., and Uzu, G.: Discovering oxidative potential (OP) drivers of atmospheric PM<sub>10</sub>, PM<sub>2.5</sub>, and PM<sub>1</sub> simultaneously in North-Eastern Spain, *Sci. Total Environ.*, 857, <https://doi.org/10.1016/j.scitotenv.2022.159386>, 2023.
- Weber, S., Uzu, G., Calas, A., Chevrier, F., Besombes, J. L., Charron, A., Salameh, D., Ježek, I., Močnik, G., and Jaffrezo, J. L.: An apportionment method for the oxidative potential of atmospheric particulate matter sources: Application to a one-year study in Chamonix, France, *Atmos. Chem. Phys.*, 18, 9617–9629, <https://doi.org/10.5194/acp-18-9617-2018>, 2018.

Weber, S., Uzu, G., Favez, O., Borlaza, L., Calas, A., Salameh, D., Chevrier, F., Allard, J., Besombes, J. L., Albinet, A., Pontet, S., Mesbah, B., Gille, G., Zhang, S., Pallares, C., Leoz-Garziandia, E., and Jaffrezo, J. L.: Source apportionment of atmospheric PM10 oxidative potential: Synthesis of 15 year-round urban datasets in France, *Atmos. Chem. Phys.*, 21, 11353–11378, <https://doi.org/10.5194/acp-21-11353-2021>, 2021.

Zhang, Y., Albinet, A., Petit, J. E., Jacob, V., Chevrier, F., Gille, G., Pontet, S., Chrétien, E., Dominik-Sègue, M., Levigoureux, G., Močnik, G., Gros, V., Jaffrezo, J. L., and Favez, O.: Substantial brown carbon emissions from wintertime residential wood burning over France, *Sci. Total Environ.*, 743, <https://doi.org/10.1016/j.scitotenv.2020.140752>, 2020.